FRACTIONATION OF THE METASTABLE EQUILIBRIUM SOLUBILITY DISTRIBUTION OF CARBONATED CALCIUM HYDROXYAPATITE

by

Shane J. Colby

A thesis submitted to the faculty of
The University of Utah
in partial fulfillment of the requirements for the degree of

Master of Science

Department of Pharmaceutics and Pharmaceutical Chemistry

The University of Utah

August 2006

THE UNIVERSITY OF UTAH GRADUATE SCHOOL

SUPERVISORY COMMITTEE APPROVAL

of a thesis submitted by

Shane J. Colby

This thesis has been read by each member of the following supervisory committee and by majority vote has been found to be satisfactory.

Steven E. Kern

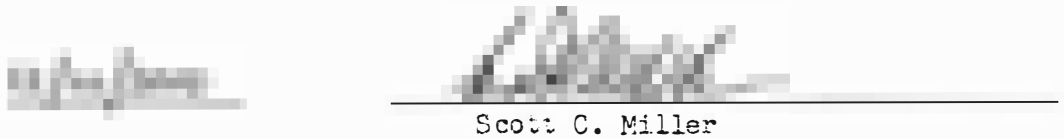

Scott C. Miller

THE UNIVERSITY OF UTAH GRADUATE SCHOOL

FINAL READING APPROVAL

To the Graduate Council of the University of Utah:

I have read the thesis of Shane in its final form and have found that (1) its format, citations, and bibliographic style are consistent and acceptable; (2) its illustrative materials including figures, tables, and charts are in place; and (3) the final manuscript is satisfactory to the supervisory committee and is ready for submission to The Graduate School.

1/12/2006

Approved for the Major Department

Approved for the Graduate Council

David S. Chapman
Dean of The Graduate School

ABSTRACT

The physical-chemical behavior of calcium hydroxyapatites in various mineralizing and demineralizing conditions has been studied for decades with the purpose of discovering its intrinsic influence on the mechanisms and extent of diseases of biologic hard tissue. There has been an assumption that thermodynamic equilibrium is reached in these experiments.

All biologic and synthetic calcium apatites studied so far in our laboratory have, however, not shown the expected results of reaching thermodynamic equilibrium. Instead, they have shown a distribution of the metastable equilibrium solubility (MES) phenomenon. That is, on a time scale of months or less, a given biomineral does not reach thermodynamic equilibrium in partially saturated solutions but rather has a distribution of apparent solubilities—more properly, a distribution of metastable equilibrium solubilities.

This thesis interprets the MES phenomenon in terms of mineral properties such as crystal morphology, specific surface area, microstrain, crystallite size, and carbonate content. In dissolution studies of constant solution composition, with a carbonated calcium hydroxyapatite (5.0 weight percent carbonate), it was found that 1) pits are formed in the apatite crystals when exposed to severe undersaturation conditions, 2) values of MES correlate with microstrain but not with crystallite size, 3) the carbonate

content (and c-axis parameter) of the mass which remains after dissolution has occurred is less than that of the original mass, 4) the specific surface area increases, and the crystallite size decreases, with dissolution. It was concluded that the dissolution behavior of bulk calcium apatite is related to the linear and independent dissolution behavior of its component domains.

This thesis secondarily evaluates the published value of the thermodynamic solubility product, $K_{sp,HAP}$, of the U.S. Government's standard for calcium hydroxyapatite, Standard Reference Material 2910. The $K_{sp,HAP}$ claimed for this material is $10^{-117.4}$. However, this value is consistent with the MES of only the more-soluble 10% of the material. The mean pK_{HAP} of the material is less soluble by several pK units than the reported $pK_{sp,HAP}$.

CONTENTS

LIST OF FIGURES

LIST OF TABLES

ACKNOWLEDGMENTS

My experience in the Department of Pharmaceutics and Pharmaceutical Chemistry at the University of Utah was made at once richer and dearer by the following individuals and groups.

Thanks to Dr. William I. Higuchi and the late Dr. Jeffrey L. Fox for inspiring me and being my mentors. You patiently gave me support, opportunity, and a scientific education. I will always be grateful.

Thank you, Drs. Steven E. Kern and Scott C. Miller, for your time, understanding, interest, and suggestions.

Thank you, Zeren Wang, for being my friend and motivating me to study pharmaceutics. You had no intellectual weakness, and you were the hardest-working man I ever had met.

Thank you, Jer Hsu, Arif Baig, Hong Zhuang, Anil Chhettry, Anthony Barry, Dustin Heslop, and Guang Yang, for being objective in giving and accepting scientific criticism, and for sharing my graduate-school experience with me. I could not have asked for better lab mates. I very much enjoyed our conversations together.

Thank you, faculty of the department, for introducing me to the study of pharmaceutics.

Thank you, National Institute of Dental Research, for providing funding to continue this work (Grant No. DE06569).

1. INTRODUCTION

The study of carbonated calcium apatite has implications in understanding and treating diseases of biologic hard tissue since carbonated calcium apatite is the principal component[1] of biologic minerals such as teeth and bone. *In vitro* solubility studies of apatite phases have been used to investigate the physical-chemical mechanisms of biomineral diseases such as dental caries and osteoporosis. Furthermore, by using carbonated apatite in situ, the interplay of biologic and physical-chemical factors can be studied.

Pure calcium hydroxyapatite (HAP), sans carbonate, was the first synthetic model for natural calcium apatite.[2-5] Conspicuously, there has been a plurality of published K_{sp} values for HAP.[2,3,6-12] On a concentration basis, they range from 0.4 to 30 mM. This situation is problematic for researchers who, in their own studies, need quantification of the proper driving force for the dissolution of HAP. Which of these K_{sp} values is correct? Which of these K_{sp} values is useful?

Historically, apatite has been treated as a pure solid, which comes to thermodynamic equilibrium in the medium that bathes it. However, the claim of this laboratory is that thermodynamic equilibrium is not reached by calcium apatites in buffers during time scales on the order of months.[13] Instead, we proposed that a metastable state is reached. Results of numerous studies of biological and synthetic carbonated calcium apatites by us[14] and others[15] have been consistent with our

laboratory's metastable equilibrium solubility (MES) hypothesis of calcium apatite solubility behavior.

The MES hypothesis arises from two general observations: 1) When apatite is exposed to partially saturated demineralization solutions, a metastable, nonequilibrium state is reached within days in which neither further measurable dissolution nor precipitation occurs. 2) Apatite exhibits a distribution of MES; that is, a single solubility value does not and cannot completely characterize the behavior of a given apatite preparation because apatite contains domains of different metastable equilibrium solubilities.

Furthermore, the surmise of this laboratory was that the domains, which compose a sample of bulk apatite, were independent of each other, and had metastable equilibrium solubilities which were functions of crystallinity.[16] An investigation into these hypotheses was made, and research was done to describe the MES phenomenon in terms of measurable quantities.

Statement of the Problem

If achieving MES is a universal phenomenon of all calcium hydroxyapatites, then it should not apply only to the carbonated calcium hydroxyapatites that have already been studied in this laboratory, but also to any noncarbonated calcium apatite, including the official U.S. government's standard reference material for calcium hydroxyapatites. This study tested the MES hypothesis with Calcium Hydroxyapatite (NIST SRM 2910), a noncarbonated apatite. A suspension of the apatite powder (10 mg/L) was continuously stirred in 0.1 M acetate buffers (pH 5; μ = 0.5 M) that contained calculated amounts of

calcium and phosphate. Each buffer was prepared to have a specific solution ion activity product (IAP) with respect to calcium hydroxyapatite stoichiometry: $Ca_{10}(PO_4)_6(OH)_2$. Different solution pIAPs (114–129), and equilibration periods (≥ 2 days) were investigated. Ca and PO_4 photometric analyses were performed on undissolved residues to determine amounts dissolved during any particular experiment.

If bulk samples of calcium hydroxyapatite are indeed composed of independent domains of varying MES, then these domains should be separable. Furthermore, if the mean MES of bulk calcium hydroxyapatite correlates with its microstrain, then the mean MES of fractions, which compose the bulk apatite, should also correlate with their microstrain. The purpose of the present study was to test this hypothesis, and to obtain experimental data that could both give insight into the MES phenomenon and to help relate the MES distributions of apatites to their crystal properties. A carbonated apatite (CAP) was synthesized and initially exposed for 2 days under stirring to 0.1 M acetate buffers (pH 5; μ = 0.5 M) that contained calculated amounts of calcium and phosphate. Each buffer was thus characterized by its solution ion activity product (IAP) with respect to the stoichiometry of hydroxyapatite. Total calcium and phosphate photometric analyses were performed on undissolved residues to determine amounts dissolved. The fraction of the apatite that dissolved in a particular buffer depended on the solution IAP. Specific undissolved residues were collected and reequilibrated for another 2 days in a fresh series of partially saturated solutions.

2. MATERIALS AND METHODS

Calcium hydroxyapatites

Five grams of Standard Reference Material® 2910 were purchased from the National Institute of Standards & Technology. This standard reference material "is intended primarily for use in evaluating the physical and chemical properties of calcium apatites of biological, geological, and synthetic origins."[17] It was synthesized by solution reaction of calcium oxide and phosphoric acid. The entire *Certificate of Analysis* of the hydroxyapatite standard can be found at https://srmors.nist.gov/view_cert.cfm?srm=2910.

The carbonated apatite of the study was prepared by a precipitation method. Aqueous $Ca(NO_3)_2$, NaH_2PO_4, and $NaHCO_3$ were added drop-wise into a 4-L reaction flask containing water maintained at 95 °C. The contents were then digested for 2 hours. The pH was held at 9.0 ± 0.1 by addition of NaOH. The result was precipitation of ~6 g of carbonated apatite (CAP). The weight percent of carbonate ion in the sample was determined to be (5.0 ± 0.3)% by the Conway Microdiffusion Method. See "Powder Residue Characterization, Carbonate Content" below.

Dissolution media: Metastable Equilibrium Solubility (MES) Solutions

Buffered solutions (0.1 M acetate ion, 0.5 M ionic strength, pH 5) were prepared with calculated amounts of aqueous stock solutions of $CaCl_2$, NaH_2PO_4, NaCl, sodium acetate, and HCl. The equilibrium calculations[18] were done with EQUIL from

MicroMath Scientific Software, Inc. HCl was defluoridated by diffusion of hexamethyldisiloxane, and the other stock solutions were defluoridated by treatment with commercial hydroxyapatite (Bio-Rad Laboratories). Each prepared buffer was distinguished by its solution ion activity product with respect to the stoichiometry of hydroxyapatite: $Ca_{10}(PO_4)_6(OH)_2$.

MES-determination experiments

Ten-mg samples of the carbonated apatite were equilibrated at 30 °C in a series of MES solutions in 500-mL glass beakers with Teflon-coated stir bars. What remained undissolved after 2 days was filtered with a 0.22-μm membrane. The net amount that dissolved into the MES solutions was determined by calcium and phosphate photometric analyses of the undissolved residue (Perkin-Elmer or Cary spectrophotometers). Plots were then made of the fraction dissolved versus the $-\log_{10}$ of the ion activity product, with respect to hydroxyapatite (HAP), of the demineralizing solution, i.e., pI_{HAP}.

Small slurry densities were purposely used so that the solution composition remained essentially constant even if dissolution took place.

For Sample SRM 2910, the MES-determination experiments were identical to those of the carbonated apatite except that 10-mg samples of the hydroxyapatite were equilibrated in 1000-mL glass beakers. Since SRM 2910 was less soluble than the CAP, a smaller slurry density was used for the experiments to ensure that the composition of the demineralizing solutions also remained constant even if dissolution took place. Similarly, what remained undissolved after 2 to 71 days was collected by filtration through a 0.22-μm membrane.

Powder residue collection

Carbonated apatite that remained undissolved after equilibration in the demineralizing solutions (80 mg powder per 4 L solution) was collected by filtration through a membrane as described above. The filter cake was dried overnight at 60 °C in an oven. Enough powder was collected similarly and pooled so that reequilibrations, X-ray diffraction, specific surface area, SEM, and carbonate assays could be performed with the residues.

Powder residue characterization

X-ray diffraction analysis

The X-ray diffraction profiles of the original apatite and its three undissolved residues were obtained by scanning over the range 20° to 90°, with a 0.02 ° step size at 10 sec/step. Staff of the Department of Metallurgical Engineering, University of Utah, performed the scans. The equipment used 40 kV, 40 mA, and had a graphite monochromator with 0.1 mm detector slit. ASCII files of the raw X-ray diffraction data, including the background, were used to obtain crystallite size, lattice, and microstrain parameters of the samples via Rietveld analysis. Dr. Arif A. Baig, University of Utah, performed the data treatment.

Specific surface area determination

Adsorption and desorption of nitrogen gas in a helium carrier onto the carbonated apatite was performed with Monosorb (an automated direct-reading surface-area analyzer

from Quantachrome Corporation). The instrument used the BET[19] method to calculate the specific surface area.

Morphology

Scanning electron micrograph (SEM) pictures of the residues were taken at the Department of Materials Science and Engineering, University of Utah.

Carbonate content

The weight percentage of the carbonate ion in the powder samples was determined by titration with hydrochloric acid. Carbon dioxide released from the annihilation of the powder by perchloric acid diffused into a chamber of barium hydroxide. This chamber was then titrated.

3. THE METASTABLE EQUILIBRIUM SOLUBILITY BEHAVIOR OF NIST SRM 2910, CALCIUM HYDROXYAPATITE

Introduction

Understanding the dissolution behavior of apatite phases has potential clinical impact in treating osteoporosis and dental caries. However, apatite is a peculiar material and poses certain challenges: 1) Values of apparent apatite solubility can be compromised even by the presence of unintended, extremely low levels of solution fluoride.[20,21] 2) The proper stoichiometry with which to interpret apatite solubility data depends strongly on solid properties,[22] as well as on solution composition.[21,23-25] 3) Apatite exhibits metastable equilibrium solubility (MES) phenomena.

MES refers to the repeatable observation that a given mass of calcium apatite (e.g., human dental enamel, rat bone,[26] synthetically prepared apatite, etc.) rapidly reaches a metastable state in partially saturated demineralizing solutions. In this state, neither measurable precipitation nor further dissolution occurs; that is, the system has not reached thermodynamic equilibrium. (At thermodynamic equilibrium, when the chemical potential of every component is constant throughout the system, regardless of the phase it is in, precipitation and dissolution rates are equal, opposite, and nonzero.) Furthermore, a given mass of apatite exhibits this metastable state over a range of solution activities. Thus, the mass of apatite exhibits a distribution of MES. The

distribution of MES lasts for at least months and can be noticed within hours after beginning the dissolution experiment. These observations would not be expected if apatite were composed of homogeneous crystals in true equilibrium with their aqueous environment.

Since the treatment and prevention of dental caries and osteoporosis may be facilitated by understanding the physical chemistry of the biomineral, this laboratory is investigating the role that the MES distribution of the biomineral plays in its behavior under both diseased and normal conditions.

Apatite MES has been studied and exploited in our laboratory since 1993. The MES concept has been remarkably successful in 1) discovering the correlation between apatite MES and the microstrain component of crystallinity[14,16,27]; 2) elucidating the stoichiometry which governs apatite solubility in various aqueous systems[21-25]; 3) investigating the effects of heat-treatment on apatite solubility[28]; and 4) describing and modeling powder and pellet dissolution in a wide range of solution conditions.[29]

This chapter presents a test of the hypothesis that even a highly crystalline, well-characterized apatite would exhibit MES. The hydroxyapatite reference material from the National Institute of Standards & Technology was deemed appropriate for this purpose. Figure 1 presents the X-ray diffraction pattern of this sample. Also, the significance of the reported K_{sp} of this sample was examined by applying the MES concept.

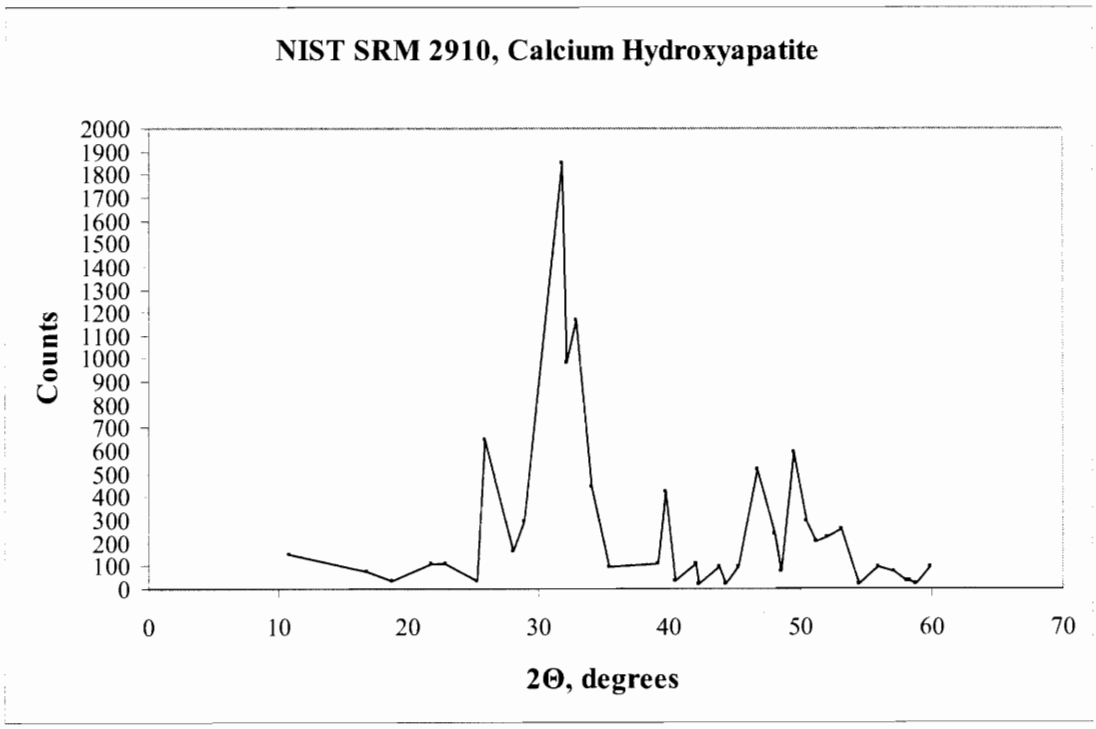

Figure 1. Outline of the X-ray diffraction pattern of NIST SRM 2910, Calcium Hydroxyapatite.

Results and discussion

To emphasize the findings of this study, consider first the possibility that the hydroxyapatite (HAP) is given time to absolutely reach thermodynamic equilibrium when placed in a series of partially saturated solutions of finite volume sufficiently large so that the solution ion activity product is insensitive to any dissolution that occurs. It will be assumed that the reported K_{sp} of the HAP ($10^{-117.4}$) is its thermodynamic K_{sp}. Figure 2 illustrates the outcome of this thought experiment. The abscissa is the initial solution ion activity product with respect to HAP.

In this thought experiment, several 10-mg samples of the HAP are initially placed into 1-L beakers of partially saturated solutions. What is seen at solution activities less than the K_{sp} of the solid is not surprising: equilibrium cannot be established in large volumes of undersaturated buffers, hence all of the 10-mg samples of the HAP dissolves.

At the solution ion activity product corresponding to the K_{sp} of the solid, it is seen that zero net percent of the HAP dissolves, a straightforward consequence of being at equilibrium. (In the equilibrium state, the magnitude of the dissolution rate is equal to the magnitude of the precipitation rate, and hence there is no net loss or gain of mass.)

At solution ion activity products larger than the K_{sp} of the solid, precipitation of HAP occurs until the solution ion activity product is reduced to and maintained at that which corresponds to the K_{sp} of the solid. The negative "net percent dissolved" values signify an increase in mass due to precipitation or crystal growth.

However, the expected results of the equilibrium state of the thought experiment presented in Figure 2 are not corroborated by experiment! When this experiment was actually conducted, the real data could not be reconciled with the achievement of

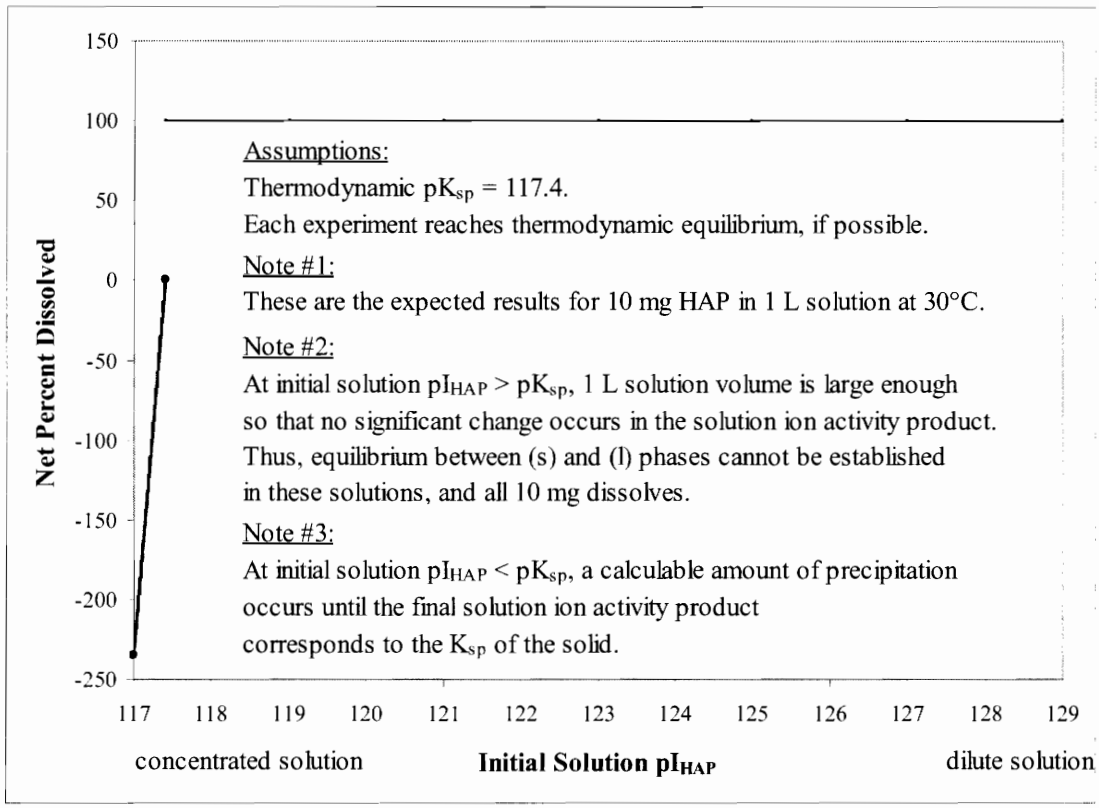

Figure 2. Results of the thought-experiment hypothesis: NIST SRM 2910, calcium hydroxyapatite, reaches thermodynamic equilibrium.

thermodynamic equilibrium, but rather with the achievement of MES, metastable equilibrium solubility.

Figure 3 presents the actual experimental data of 2 to 71 days' equilibration time. Each symbol represents an independent experiment in a particular solution of essentially constant ion activity product. Vertical error bars (which imply reproducibility) are ± 5 ordinate units. Because of the large volumes of solution, the horizontal error bars are small.

Little of the sample dissolved in the most concentrated solution (pI_{HAP} = 114) whereas most of it dissolved after equilibrating in the most dilute solution (pI_{HAP} = 129). Figure 3, the metastable equilibrium solubility (MES) distribution of the sample, can be interpreted in the following way: In a solution of essentially constant solution ion activity product, dissolution occurs of the more reactive parts of the 10-mg bulk HAP sample. Dissolution ends, and MES is reached, when the remaining, less-reactive parts are in a metastable state with respect to the solution and to each other.

Even after 71 days of equilibration time (Figure 3; solid square symbols), the MES profile of the HAP has changed little. Thus, the MES state appears to be already established at 2 days and lasts for at least 71 days. This result is not really surprising: This HAP sample is like all other apatite materials we have studied in that it does not behave as a single, well-defined crystalline material of a single, rapidly established, thermodynamic solubility.

As a practical matter, due to the experimental hysteresis possible by choosing initial solution activities larger or smaller than the theoretical K_{sp} value (see Figure 2), and then changing the solution ion activity product by the addition of sufficient calcium,

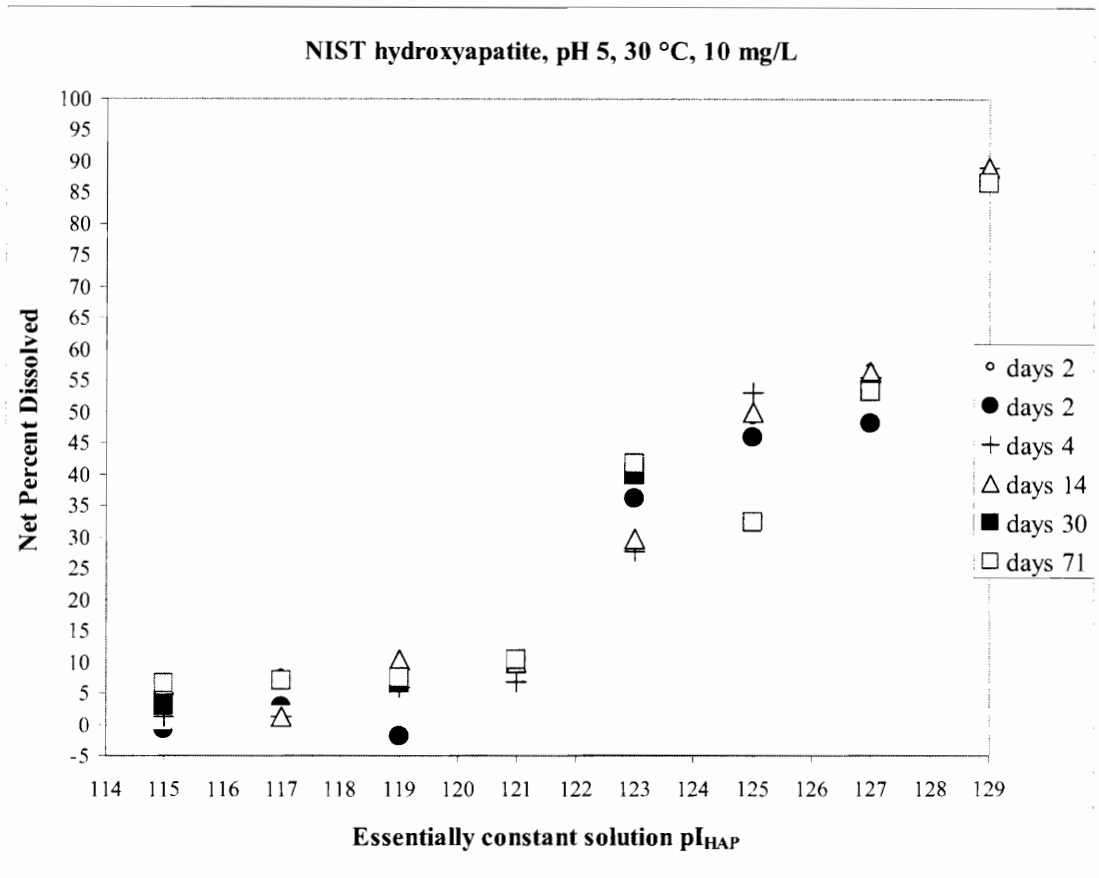

Figure 3. Actual experimental results: NIST SRM 2910, calcium hydroxyapatite, reaches MES, metastable equilibrium solubility.

phosphate, or hydroxide ions, it is reasonable that crystals have a finite distribution of apparent K_{sp} due to the degree of supersaturation necessary before phase changes occur.

Now let us turn our attention to an analysis of the reported K_{sp} of the NIST HAP sample, $pK_{sp.HAP} = 117.4$. According to the *Certificate of Analysis* of this sample, the K_{sp} was determined by equilibrating ~400 mg of the HAP in 20 mL phosphoric acid solution at 37 °C for 60 days after which solution calcium and phosphate concentrations as well as pH were measured. The final solution ion activity product was calculated to be $10^{-114.7}$ by which the K_{sp} was deduced. The significance of the NIST K_{sp} value can be seen in light of the MES data presented in Figure 3.

Note first that one variable that affected the reported K_{sp} is the duration of the solubility-determination experiment. The NIST experimenters equilibrated the HAP for 60 days in a continuously shaken water bath. However, since the metastable state for this sample still existed at 71 days, 60 days is clearly not enough time to reach thermodynamic equilibrium. Thus, the reported K_{sp} value cannot be a thermodynamic quantity.

NIST's slurry density is 2000x as large as that used to obtain the results of the MES experiments. In NIST's experiment, after a small amount of dissolution, the solution goes from only being a phosphate common-ion solution to being partially saturated with respect to HAP ($pI_{HAP} = 117.4$). From Figure 3, however, we see that ~90% of the bulk HAP sample is in a metastable state in the solution of pI_{HAP} 117.4. The remainder is more soluble and dissolves because it has an MES solubility product greater than $10^{-117.4}$. So the reporting by NIST that the pK_{sp} of the HAP is 117.4 is consistent with the metastable equilibrium solubility of just 10% of the bulk material. It is

interesting to consider that according to NIST, the HAP contains a "crystallographically disordered material fraction of 9.1% ± 4.1%."[17]

In essence, the large slurry density biases the reported K_{sp} toward a higher value. The reported K_{sp} is really an "apparent" K_{sp} of just ~10% of the bulk material, due to the conditions of the experiment. Therefore, we believe that the best way to characterize the solubility behavior of an apatite is to characterize its MES behavior. Equilibrium is not the proper perspective with which to interpret apatite data!

Conclusions

The fraction of the apatite (Standard Reference Material® 2910) that dissolved decreased with increasing solution ionic activity product in accordance with the presence of a distribution of metastable equilibrium solubility (MES) in the sample.

Exhibition of an MES distribution by the apatite (SRM 2910) strengthens the view that a distribution of MES is a universal property of apatites.

The reported solubility product of SRM 2910 (pK_{sp} = 117.4) is consistent with measuring the metastable equilibrium solubility of the most soluble part of the sample (~10% of the bulk material). The reported K_{sp}, therefore, should not be taken as the definitive thermodynamic value.

The apparent mean MES of SRM 2910 is less soluble than the reported solubility by several pK_{sp} units.

Several questions arise after contemplating an MES profile such as Figure 3. According to these results, in any given apatite sample there exist high- and low-soluble parts. If the low-soluble parts were re-equilibrated in lesser partially saturated solutions,

would these low-soluble parts still exhibit MES? What if the low-soluble parts were re-equilibrated in higher partially saturated solutions? How high must the supersaturation be before MES is disrupted and precipitation occurs? What is the relationship between MES and kinetics of dissolution? Does the efficacy of bone cells and antiosteoporotic drugs depend in any way on the MES distribution of the biomineral? In light of these unknowns, the following work is anticipated.

Future work

To further substantiate the hypothesis that all apatitic materials exhibit MES phenomena, attempt to obtain the MES distribution profile of other apatites, including fluoroapatite, $Ca_{10}(PO_4)_6F_2$.

Fractionate bulk NIST HAP into several component fractions, each with its own MES phenomena. Fractionation may allow for an assessment of the importance of intrinsic MES on the effect of antiosteoporotic and cariostatic compounds, including fluoride.

Examine the powder dissolution kinetics of different MES fractions of the same bulk apatite. This will shed light on the surface reaction involved in dissolution as well as the relationship between reaction rate and intrinsic MES. (Earlier work suggests that surface reaction-rate constants and MES are inversely proportional.)[29]

4. EXAMINATION OF THE METASTABLE EQUILIBRIUM SOLUBILITY BEHAVIOR OF CARBONATED CALCIUM APATITE IN TERMS OF PHYSICAL PROPERTIES

Introduction

Since 1993, this laboratory has observed that calcium apatites in partially saturated solutions do not exhibit a single solubility within an experimentally reachable time frame, but rather achieve a distribution of apparent solubilities.[13] Each apatite studied has shown a distribution of this nonthermodynamic solubility phenomenon. Studied samples have included human and rat bone[30]; human enamel; commercially available hydroxyapatite; monoclinic hydroxyapatite; and hydroxyapatite or carbonated apatite synthesized by either us or by other scientists.

A distribution of "metastable equilibrium solubility" (MES) within these materials lasts for months and is established within hours of being exposed to partially saturated solutions. This distribution of the extent of dissolution of apatite has been thought of as the dissolution of a continuous mixture of independent polymorphs. Distributions of MES have been 1) Used to successfully describe and model powder and pellet dissolution in a wide range of solution conditions,[29] 2) Used as a method to test the hypothesis that surface complexes of predictable stoichiometries govern the dissolution

of apatite,[21,24] and 3) Used to assess the changes that apatite undergoes upon being heated.[28]

We believe that advances in the treatment and prevention of dental caries and osteoporosis lie in understanding the physical chemistry of the biomineral. Moreover, we believe that the MES distribution of the biomineral plays a singular role in the behavior of apatitic materials under all conditions, including those of osteoporosis and dental caries.

The interpretation of the distribution of apatitic MES in terms of crystal properties is the focus of this chapter. Experiments were designed to 1) test the hypothesis that apatites are composed of independent domains of different solubilities which are functions of crystallinity; and 2) obtain experimental data which could both give physical insight into the MES phenomenon and help relate the MES distributions of apatites to their crystal properties. The question inspired by previous work was: With what does MES correlate (morphology, crystal sizes, solubility distribution, particle-size distribution)?

As a precursor to the experimental work, the following hypotheses (H) and their consequential and testable deductions (D) were declared.

H1. Apatite is composed of independent domains of varying solubility.
D1. Apatite should be separable into independent component fractions.
D2. Bulk apatite should behave as a sum of its independent fractions.

H2. MES is a general property of all calcium apatites.
D2. MES phenomena should extend to even the fractions of apatites.

H3. The magnitude of MES is linearly determined by crystallinity.
D3. MES of independent fractions should be linearly correlated with the crystallinity of the fractions.

Mathematical development of H1: Independence and additivity of domains

Below it is assumed that the total apatite amount that dissolves ($M_{dissolved}$) when a sample of bulk apatite is exposed to a particular demineralizing solution (j) is a linear function (f) of the total (N) amounts of soluble, sparingly soluble, and insoluble domains (m_i) which compose the bulk apatite.

$$M_{dissolved,j} = f(m_1, m_2, \ldots, m_N) \tag{1}.$$

Furthermore, the amount of total dissolved apatite is assumed to be a piecewise smooth function. Its total differential is therefore

$$dM_{dissolved,j} = \sum_{i=1}^{N} \left(\frac{\partial M_{dissolved,j}}{\partial m_i} \right)_m dm_i \tag{2}.$$

The partial derivatives are taken with all domains other than m_i held constant. Here, m refers to all domains other than the integrating variable, m_i. Note that $1 \leq i \leq N$. Equation 2 can be integrated and expanded.

$$M_{dissolved,j} = \int_0^{m_1} \left(\frac{\partial M_{dissolved,j}}{\partial m_1} \right)_m dm_1 + \int_0^{m_2} \left(\frac{\partial M_{dissolved,j}}{\partial m_2} \right)_m dm_2 + \ldots \tag{3}.$$

The definite integration of the right-hand side of Equation 3 can be carried out.

$$M_{dissolved,j} = \left(\frac{\partial M_{dissolved,j}}{\partial m_1} \right)_m m_1 + \left(\frac{\partial M_{dissolved,j}}{\partial m_2} \right)_m m_2 + \ldots \quad (4).$$

Equation 4 assumes that the partial derivatives of Equation 3 are constant. Expressed differently, the effect per unit mass that a particular domain makes to the total amount dissolved does not depend on the amount of the particular domain in the apatite.

Equation 4 is next normalized to the fraction dissolved of the original apatite exposed to the particular demineralization solution, to match the form of the experimental data of the MES-determination experiments:

$$\frac{M_{dissolved,j}}{M_{total}} = \left(\frac{\partial M_{dissolved,j}}{\partial m_1} \right)_m x_1 + \left(\frac{\partial M_{dissolved,j}}{\partial m_2} \right)_m x_2 + \ldots \quad (5).$$

Here, x_i is the weight fraction of the particular domain. $0 < x_i \leq 1$.

Equation 5 allows the following question to be answered: Is the percent dissolved of a carbonated apatite (CAP) in a particular solution a function simply of the solubility of its component domains in the same solution? In order to use this equation in its general form, the amounts of the component domains need to be known, and the domains need to be separable from each other. However, determining the potential number of conceivable domains in a bulk CAP—let alone separating them by dissolution tendency—is experimentally impractical. Instead, we can separate CAP into an arbitrary number of fractions, or collections of similarly soluble domains. Separating the insoluble from the soluble fractions of a bulk CAP by exposure to demineralization solutions was anticipated to be as elegant and direct as separating grains of sand by size.

If the weight fractions of the component fractions of a bulk CAP are not known a priori, as is the case for any biologic, or unstudied CAP, Equation 5 has utility in a special form as discussed next.

Equation 5 can be used to obtain Deductions 1 and 2 of Hypothesis 1. According to the metastable equilibrium hypothesis, in a partially saturated solution in which incomplete dissolution has occurred, there exists a dissolved mass, and another undissolved mass, which is in metastable equilibrium with the solution. Equation 5 can be simplified to express this case.

$$\frac{M_{dissolved,j}}{M_{total}} = \left(\frac{\partial M_{dissolved,j}}{\partial m_{dissolved}} \right)_{un} x_{dissolved} + \left(\frac{\partial M_{dissolved,j}}{\partial m_{un}} \right)_{dissolved} x_{un} \tag{6}.$$

Here, the subscript *un* implies "undissolved."

By inspection, Equation 6 can be rewritten as

$$\frac{M_{dissolved,j}}{M_{total}} = x_{dissolved} + \left(\frac{\partial M_{dissolved,j}}{\partial m_{un}} \right)_{dissolved} x_{un} \tag{7}.$$

since the first derivative on the right-hand side is unity. Since $x_{dissolved} + x_{un} = 1$, Equation 7 can be written as

$$\frac{M_{dissolved,j}}{M_{total}} = x_{dissolved} + \left(\frac{\partial M_{dissolved,j}}{\partial m_{un}} \right)_{dissolved} \cdot (1 - x_{dissolved}) \tag{8}.$$

The applications of Equations 5 and 8 will be discussed in the "Results and Discussion" section.

A carbonated apatite was separated into fractions of different MES. The fractions were analyzed in terms of crystallinity, lattice parameters, specific surface area, and SEM morphology. The continuous MES distribution of the CAP was interpreted in terms of the continuous MES distributions of its fractions.

Additionally, according to Equation 8, the percent dissolved of the original CAP (left-hand side) depends only upon the fraction that remains (right-hand side, second term), as long as the mass of the already dissolved portion is taken into account (right-hand side, first term). This calculation was done to see if indeed a bulk CAP behaved simply as the sum of a "dissolved portion" and an "undissolved portion."

Results and discussion

The SEM photographs that follow are presented as a qualitative view of the morphology of the samples, and as a quantitative estimate of the dimensions of the crystals. Figure 4 presents the crystals of F1, the original 5.0% carbonated apatite, after being synthesized and before being exposed to any demineralizing solution. Figure 4 shows that the crystals are hexagonal, long, and smooth.

The closed circles of Figure 5 display the metastable equilibrium solubility (MES) distribution of F1. Each symbol represents an independent experiment. Invisible vertical error bars are ± 5 percentage points throughout this chapter. Little of the carbonated apatite (CAP) dissolved in the most concentrated solution of ion activity product 10^{-111} with respect to hydroxyapatite whereas most of it dissolved after equilibrating in the most

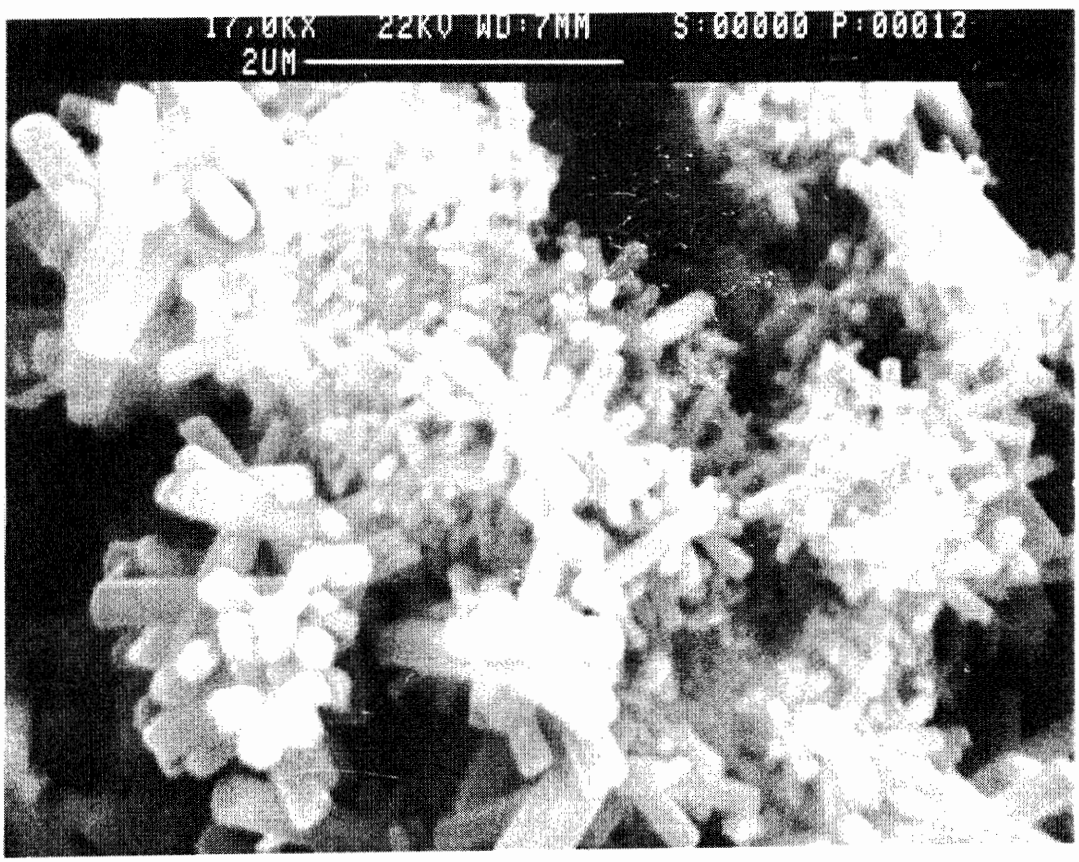

Figure 4. SEM of CAP F1: smooth, hexagonal faces.

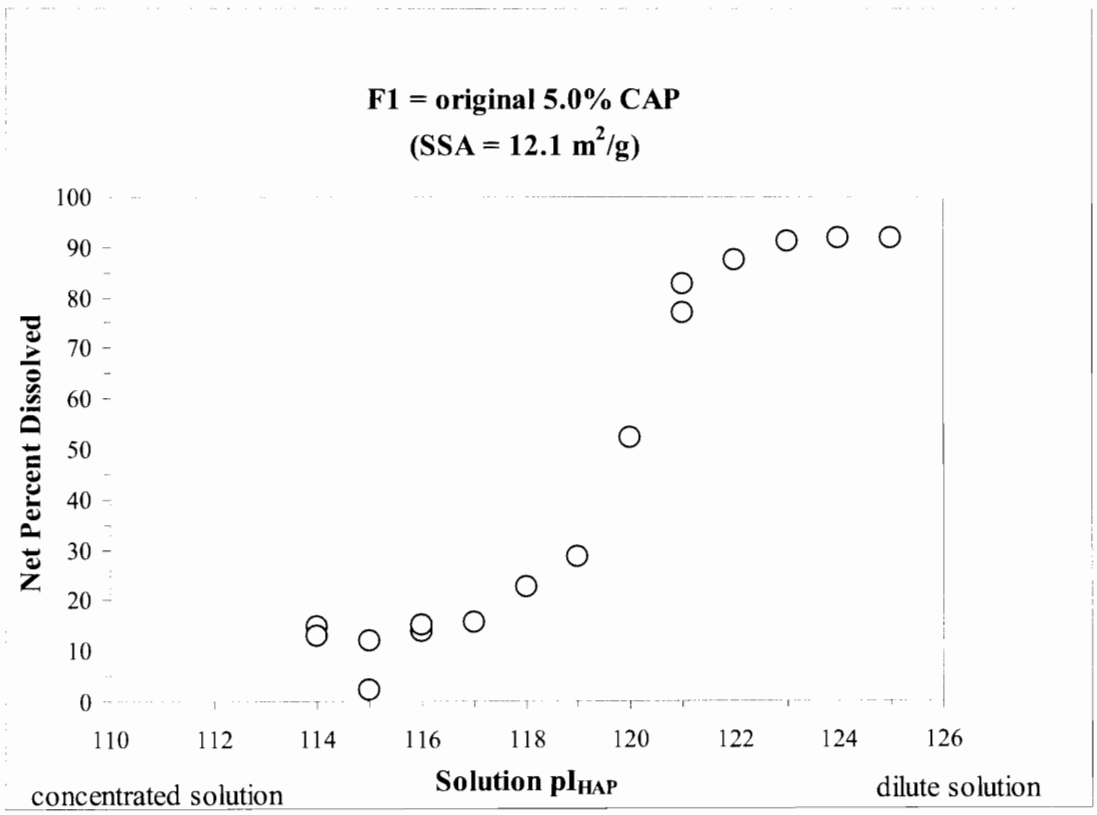

Figure 5. Two-day MES distribution of CAP F1, the original 5.0% carbonated apatite.

dilute solution (pI_{HAP} = 125). In other words, the CAP did not achieve true equilibrium, nor did it behave as a single, well-defined crystalline material of a single, thermodynamic solubility. If it did, the percent dissolved would either be < 0% (precipitation, or crystal growth), 0% (none dissolved, equilibrium reached), or 100% (all dissolved) depending on the equilibrating solution.

Several separate equilibrations of powder F1 were done in solutions of pI_{HAP} = 114. The undissolved residues of these experiments were dried, collected, and re-equilibrated in fresh solutions of pI_{HAP} ranging from 114 to 125. The SEM photograph of the F114 crystals themselves before reequilibration is presented in Figure 6. Since the difference between F1 and F114 is that F114 is what remains after ~10% of F1 has dissolved, it is not surprising that the two SEM pictures are so similar.

The open circles of Figure 7 illustrate the results of the re-equilibration of F114. The fraction dissolved of F114 is generally depressed relative to F1, the primary control. F114 was considered a secondary control because it acted as a baseline for the effects of equilibration of two days in a dissolution medium and subsequent filtering and drying operations. Evidently these operations contribute to an apparent lowering of the dissolving tendency of the material (Figure 7). As an aid to what follows, Table I presents designations and descriptions of the CAP and its three fractions used in this study.

Two other undissolved residues, F119 and F121, were also collected after the synthesized apatite, F1, had been exposed to partially saturated acetate buffers of pI_{HAP}119 and 121, respectively. Figure 8 shows the residue of F1 collected at solution pI_{HAP} 119. Dissolution traces are found down the c-axis channel[31] of the crystals.

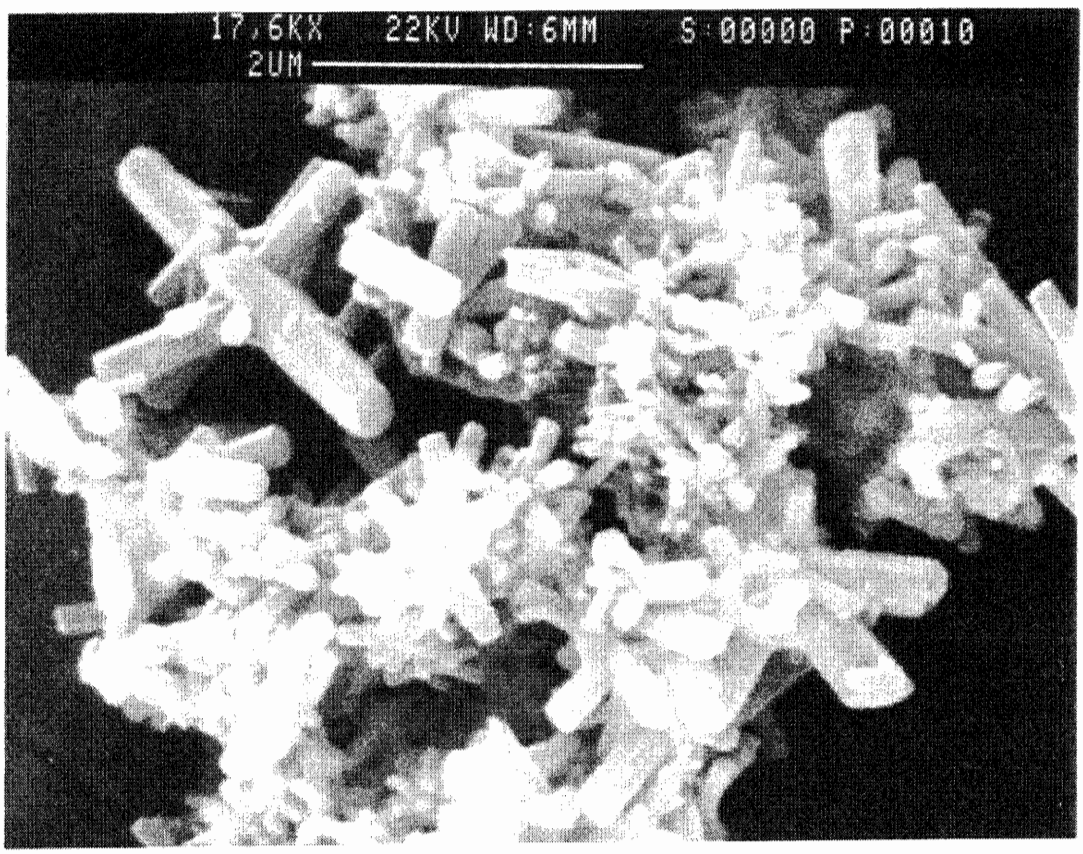

Figure 6. SEM of CAP F114, very much like the SEM of CAP F1.

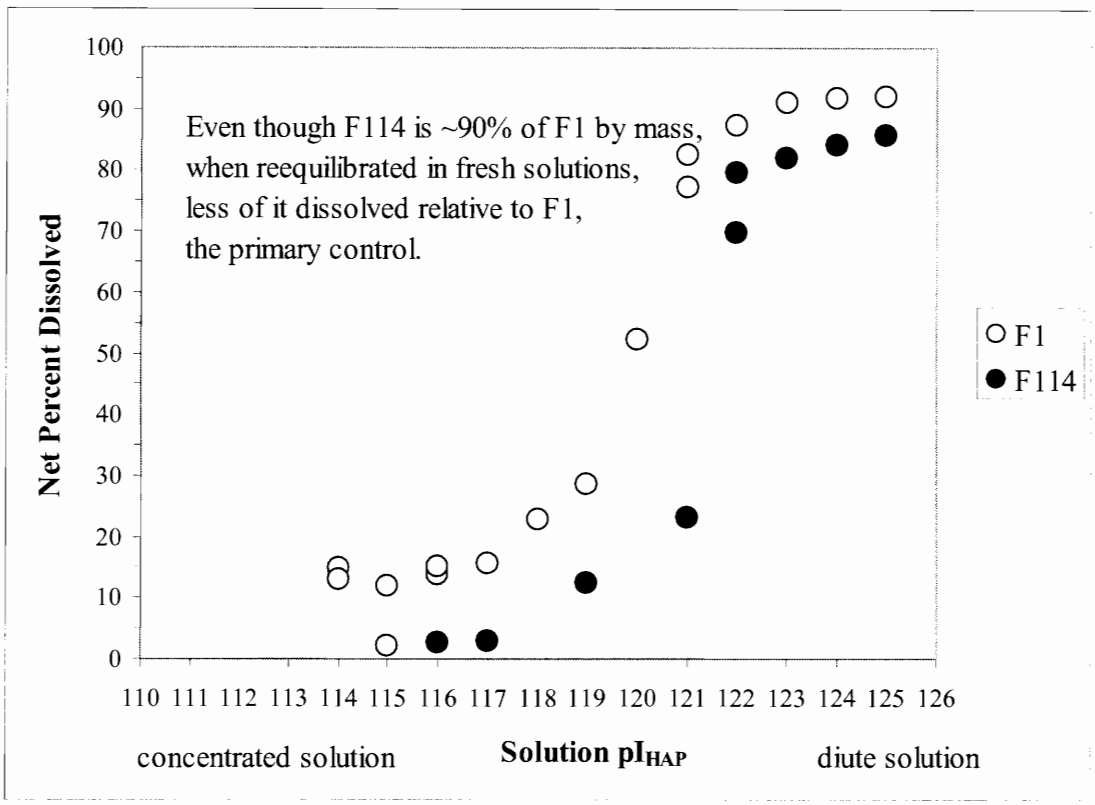

Figure 7. Two-day MES distribution profiles of CAP F1 (the primary control) and CAP F114 (the secondary control).

Table I. Abbreviations and descriptions of the carbonated hydroxyapatites.

F1

The original 5.0% carbonated apatite. The primary control.

F114

Fraction 114, 5.0% carbonate. The secondary control.
That part of F1 which remained undissolved (~ 90%)
after equilibrating 2 days in pI_{HAP} 114 solution.

F114 trans = the transformation, through Equation 8, of F114's MES data.

F119

Fraction 119, 4.0% carbonate.
That part of F1 which remained undissolved (~ 70%)
after equilibrating 2 days in pI_{HAP} 119 solution.

F119 trans = the transformation, through Equation 8, of F119's MES data.

F121

Fraction 121, 3.5% carbonate.
That part of F1 which remained undissolved (~ 25%)
after equilibrating 2 days in pI_{HAP} 121 solution.

F121 trans = the transformation, through Equation 8, of F121's MES data.

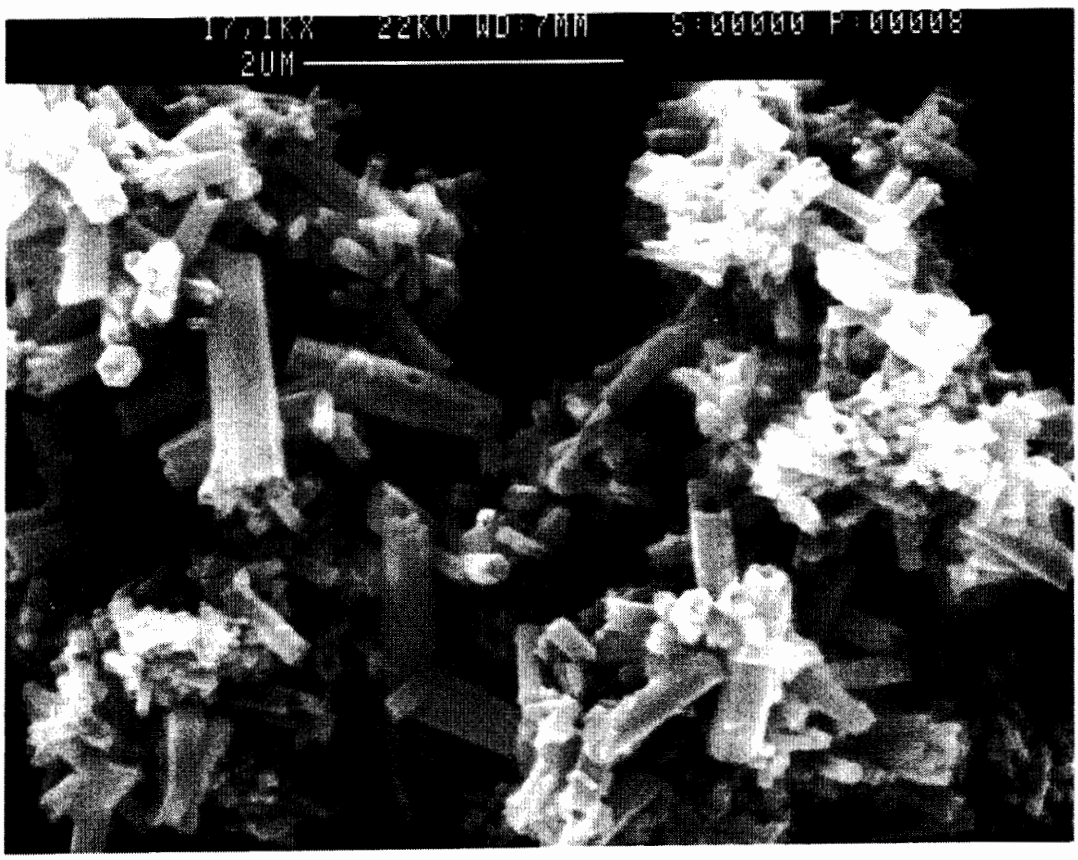

Figure 8. SEM of CAP F119: Apparent dissolution.

Figure 9 shows the results of the reequilibration experiments of F119. Figure 10 shows the effect that dissolution of F1 in pI_{HAP} 121 has had on the crystals, and Figure 11 shows the MES of these same crystals.

Figure 12 presents a summary of the MES data. Shown are the MES distributions of F1, F114, and F119 along with the partial MES distribution of F121. This figure shows that the more soluble parts of CAP F1 can be successively eliminated.

At each particular solution depicted in Figure 12, there is a portion of powder which dissolves and a portion of powder which remains. Since F114, F119, and F121 are each fractions of F1, the MES data of each of these fractions can be successively input into Equation 8, which theoretically applies in each case. If the assumptions of independent additivity of domains inherent in Equation 7 apply, then computation of the right-hand side should be within experimental error of the original data, the left-hand side. Equation 8 is repeated for convenience.

$$\frac{M_{dissolved,j}}{M_{total}} = x_{dissolved} + \left(\frac{\partial M_{dissolved,j}}{\partial m_{un}} \right)_{dissolved} \cdot (1 - x_{dissolved}) \qquad (8).$$

In Equation 8, $\frac{M_{dissolved,j}}{M_{total}}$, are the range of the F1 data of Figure 5 corresponding to the domain j $\in$ [pI_{HAP} 114..pI_{HAP} 125].

The first term of the right-hand side of Equation 8, the weight percent of the dissolved fraction at the solution where the fraction was collected (i.e., in this case pI_{HAP} 114, 119, or 121) is also obtained by inspection of Figure 5.

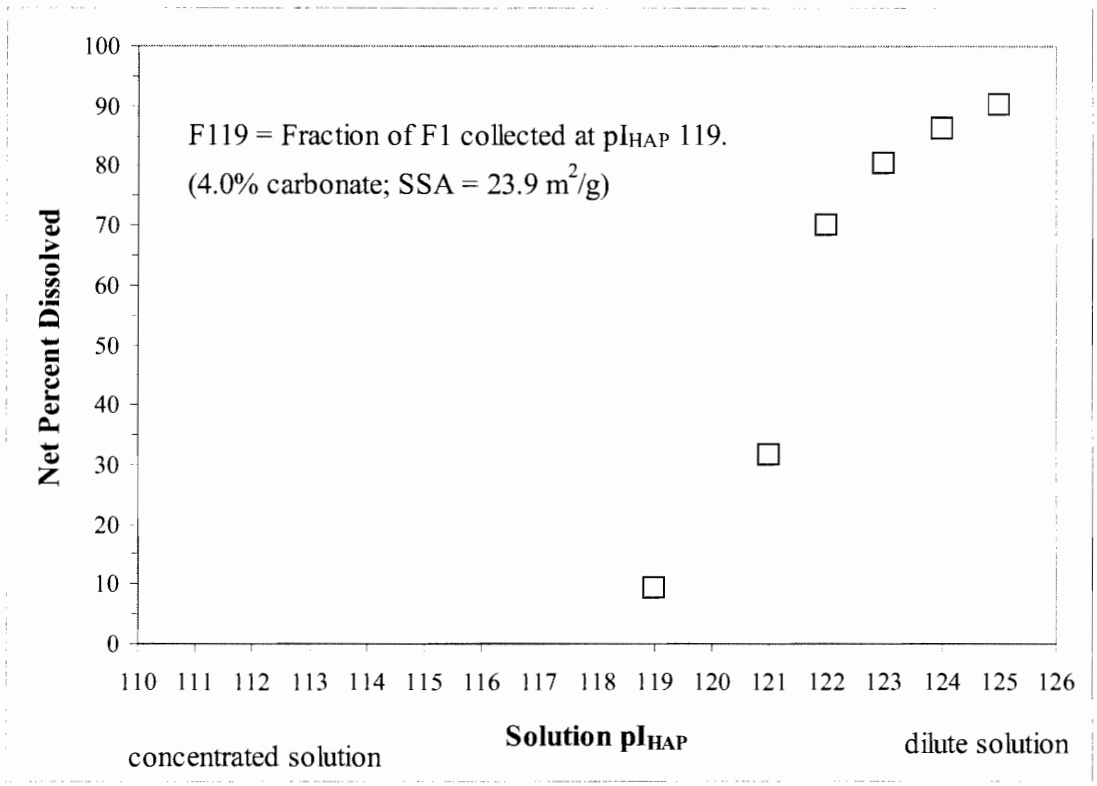

Figure 9. Two-day MES distribution profile of CAP F119.

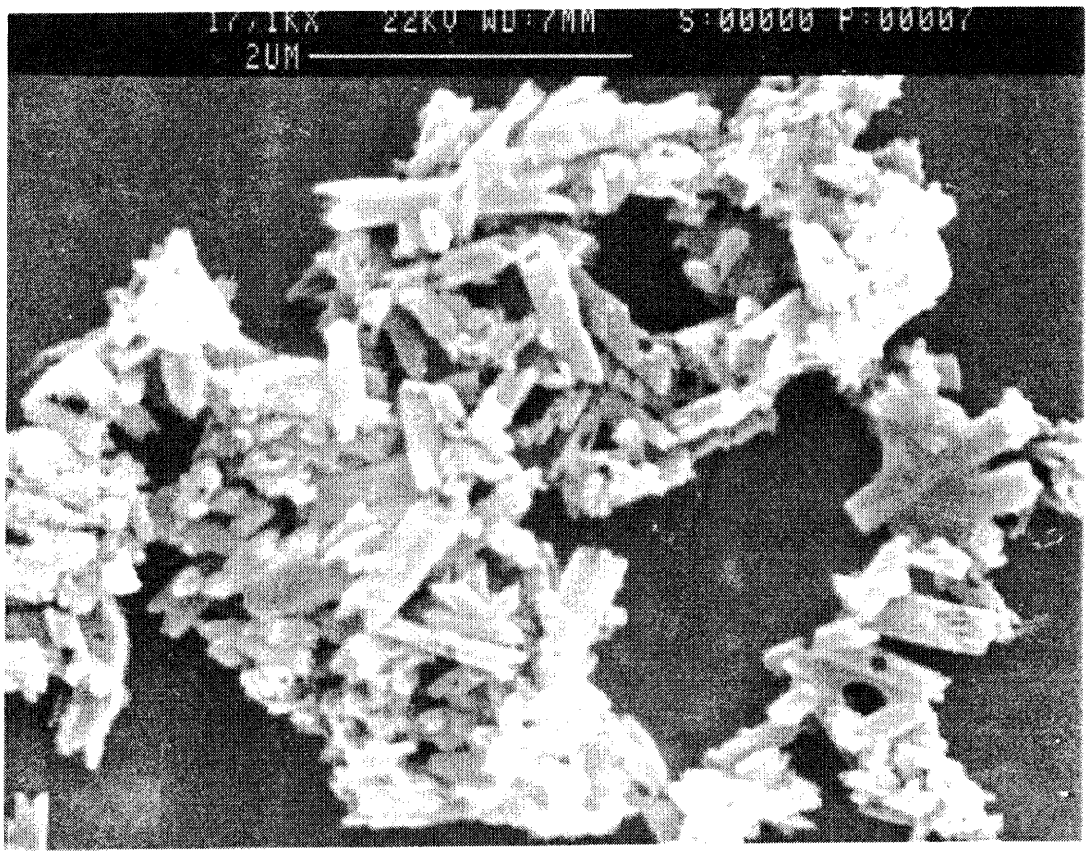

Figure 10. SEM of CAP F121: Severe dissolution.

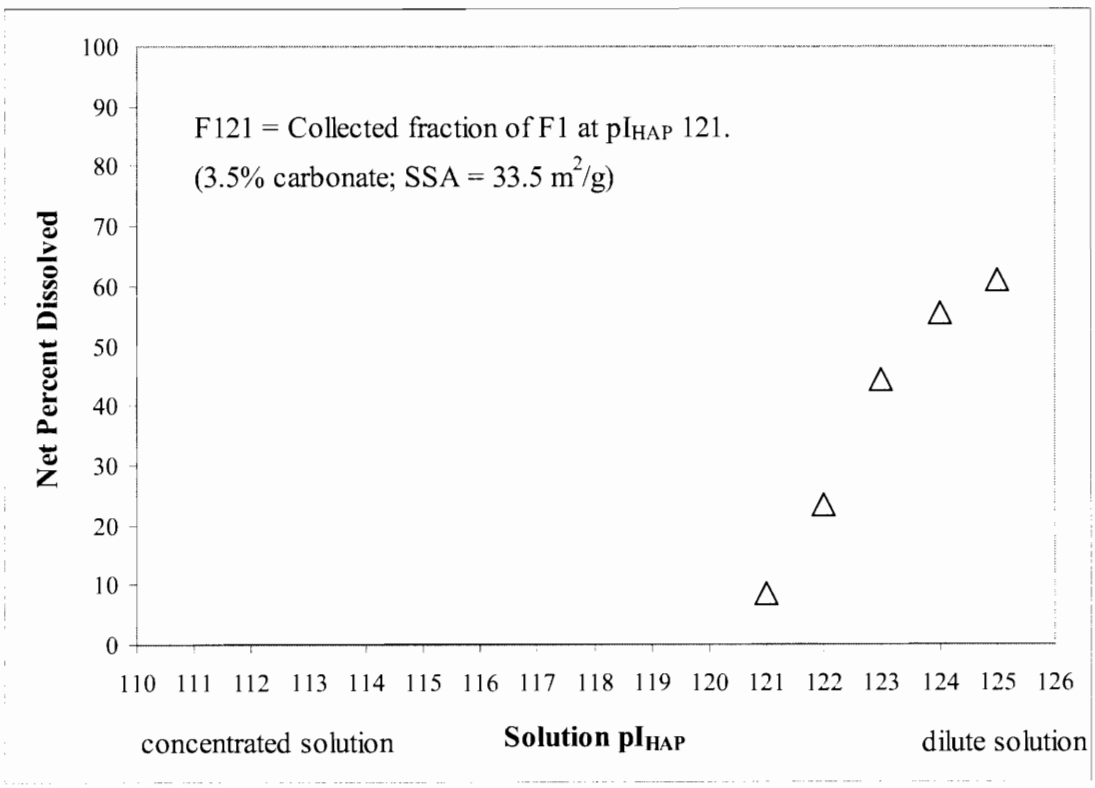

Figure 11. Two-day MES distribution profile of CAP F121.

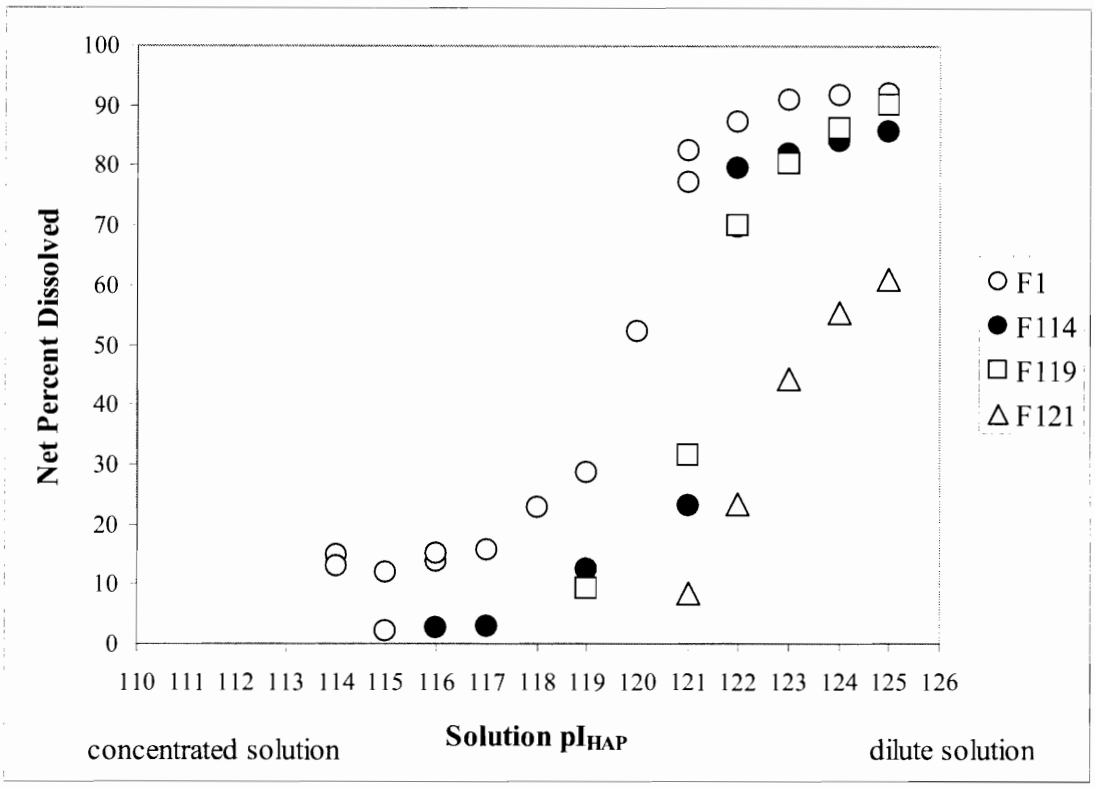

Figure 12. Combined MES distribution profile of CAPs F1, F114, F119, and F121.

The second term of Equation 8, $\left(\frac{\partial M_{dissolved,j}}{\partial m_{un}}\right)_{dissolved}$, is obtained experimentally. The undissolved residue of interest (F114, F119, or F121) is re-equilibrated in fresh MES demineralization solutions. The term is then obtained from the range of the reequilibration plots (i.e., Figures 7, 9, 11) corresponding to the solution of interest, j.

The third term of Equation 8 is the weight fraction of F1 of the residue of interest, either F114, F119, or F121.

Equation 8 was used with the MES distribution data of F114, F119, and F121. The results (F114 trans, F119 trans, F121 trans) are shown in Figure 13.

Collected residues that were re-equilibrated show their own MES distributions, which are shifted toward lower-solubility values. Relative to the original CAP, the MES distributions of the reequilibrated residues behaved simply as if the most-soluble parts of the original had been eliminated. These findings support the view that there is elimination of the most-soluble part during apatitic dissolution; and that during the time-course of MES, the fractions equilibrate solely with the dissolution medium and do not re-equilibrate with each other.

Figure 13 (dots) show that the solubility of F1 behaves like F114 in the solutions of $pI_{HAP} \geq 114$ in which everything but F114 has been eliminated through dissolution. Likewise in the same figure (solid squares), the solubility of F1 behaves like F119 in the solutions of $pI_{HAP} \geq 119$ in which all domains but the domains of fraction F119 have been eliminated through dissolution. Again, the solid triangles of Figure 13 show that the solubility of F1 behaves like F121 in the solutions of $pI_{HAP} \geq 121$ in which all fractions

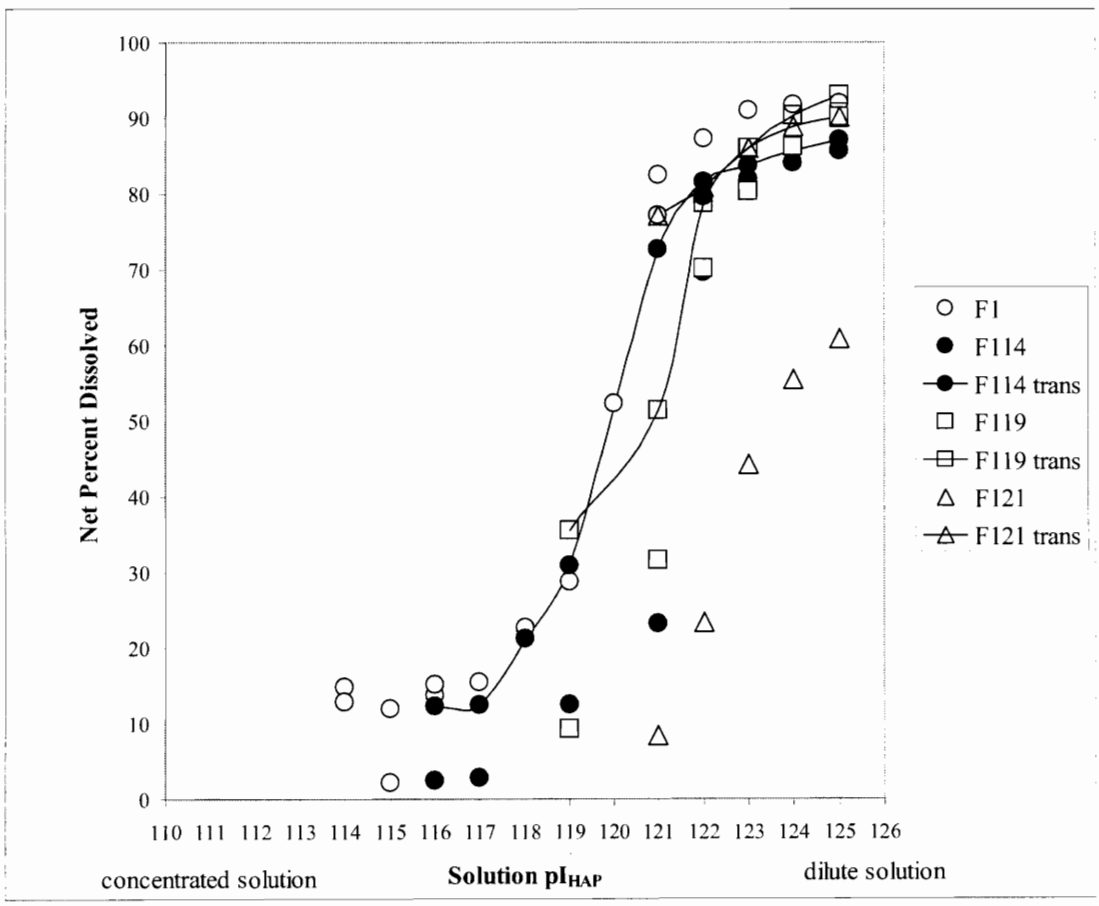

Figure 13. Combined, transformed, MES distribution profiles: CAPs F1, F114, F119, and F121.

but F121 have been eliminated through dissolution.

Figure 13 displays at once the MES distributions of the original CAP (F1) and its three residues (F114, F119, and F121). The importance of Figure 13 is three-fold:

1) The more soluble fractions of a CAP can be eliminated.

2) Each fraction continues to exhibit a distribution of MES. This is a result of the presence of varyingly soluble domains still present in each fraction.

3) The bulk CAP behaves simply like its undissolved residue. In other words, F1 showed the algebraic consequence (Equation 8) of the assumption that a given CAP preparation is a separable mixture of independent fractions of different solubilities.

The test of additivity and independence depicted in Figure 13 is not a foregone conclusion because the second, derivative term of Equation 8 is independent and unknown at the time the left-hand side is determined.

Figures 14-17 show the X-ray diffraction profiles, respectively, of F1, F114, F119, and F121. Each shows customary apatitic peaks (refer to Figure 1 as the reference standard). These data allowed calculation of crystal parameters via Rietveld analysis. Table II presents a summary of the crystallinity and specific surface area analyses performed.

Table II. X-ray diffraction and surface area results

F	mean pKHAP	X	X error	Y	Y error	a	c	SSA
1	120.0	0.15456	0.04210	0.06618	0.00828	9.4057	6.8952	12.1
114	121.0	0.11790	0.01428	0.07828	0.00866	9.4060	6.8947	12.4
119	121.5	0.07466	0.01417	0.09464	0.00881	9.4074	6.8931	23.9
121	123.5	0.04725	0.01422	0.11701	0.01018	9.4060	6.8916	33.5

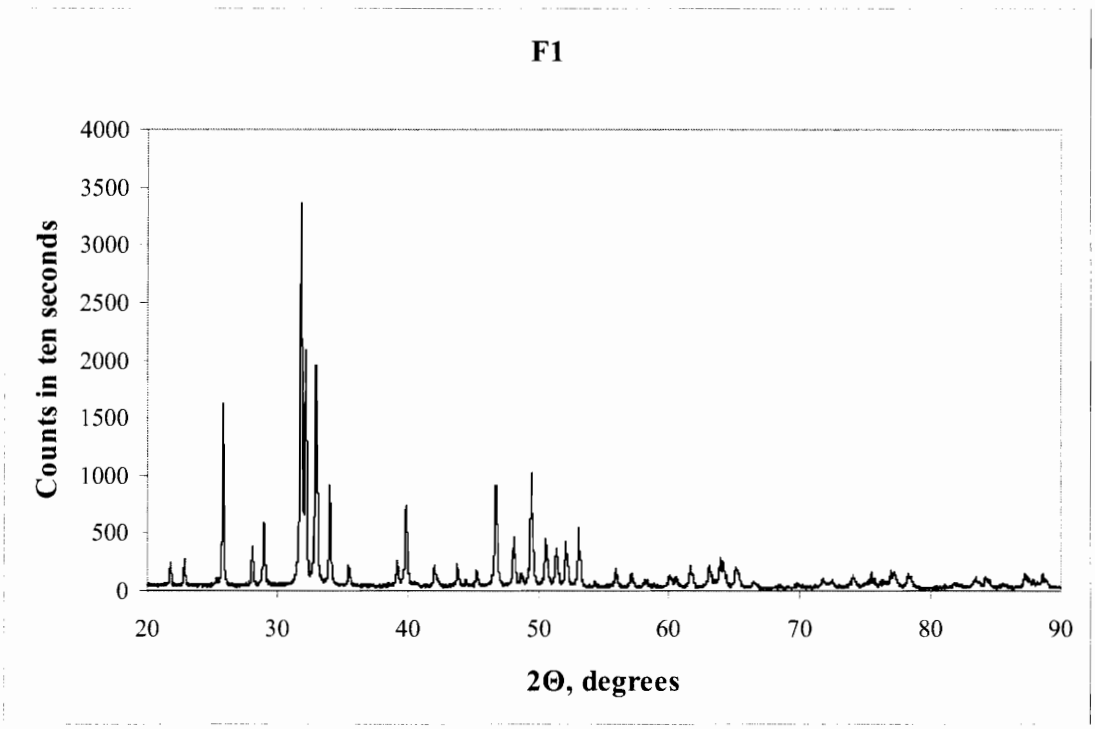

Figure 14. X-ray diffraction profile of CAP F1.

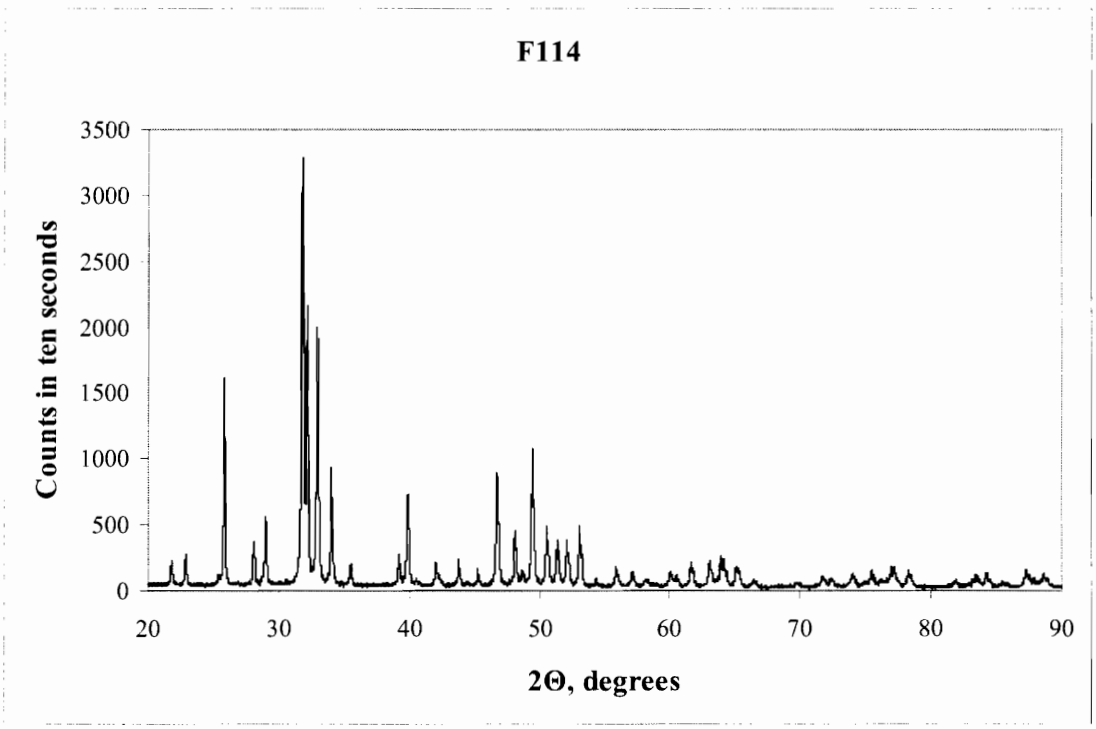

Figure 15. X-ray diffraction profile of CAP F114.

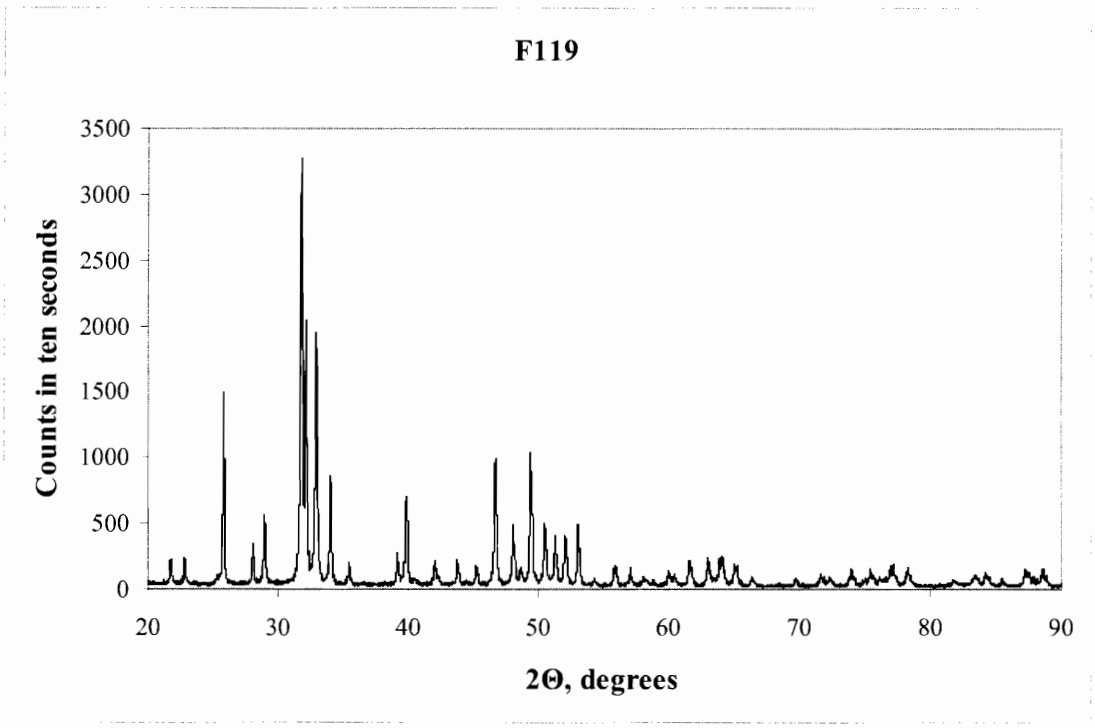

Figure 16. X-ray diffraction profile of CAP F119.

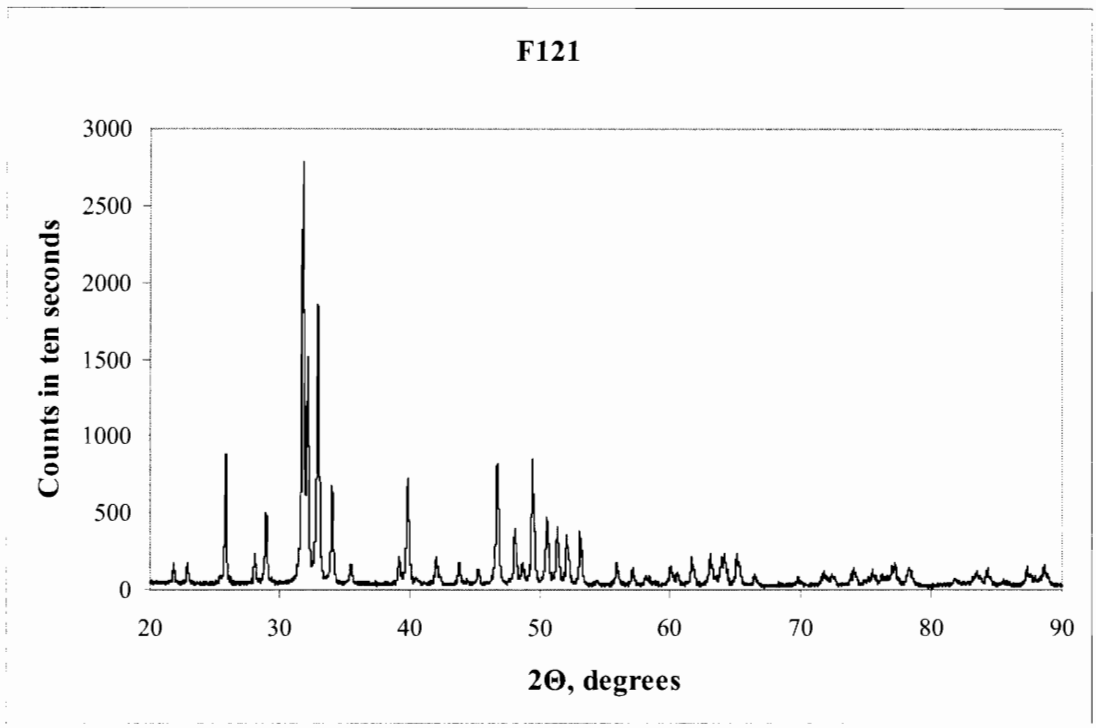

Figure 17. X-ray diffraction profile of CAP F121.

pK_{HAP}	=	the mean metastable equilibrium solubility product with respect to hydroxyapatite (HAP) stoichiometry.
X	=	microstrain parameter.
Y	=	crystallite size parameter, inversely proportional to crystallite size.
a, c	=	lattice parameters in Å.
SSA	=	specific surface area in m^2/g.

Table II, which shows an increase in specific surface area (SSA) with a decrease in crystallite size, corroborates the parameters of the Rietveld analysis as being physically meaningful. Table II also shows that SSA increases as dissolution progresses.

From Figure 12, residues F114, F119, and F121 of bulk F1 are seen to exhibit lower metastable equilibrium solubilities than F1. It has been reported[20] that solution fluoride levels as low as ~0.05 ppb can lower the extent of dissolution of apatite significantly in acetate buffers of pH 5. Since it is practically impossible to entirely remove solution fluoride, it is reasonable to ask if the shift toward lower solubility values shown in Figure 4 can be attributed to depression by solution fluoride. In other words, is there solubility depression of the material because elimination of the higher-soluble portions has been achieved, or do the reequilibrated residues dissolve less because they release adsorbed fluoride into their new equilibration solution? The importance of a possible threshold for the solution fluoride effect as well as the effect of preadsorbed fluoride has been reported elsewhere.[20,32]

The effect of the crystallinity of the different fractions on bulk apatite behavior was previously surmised only on the basis that crystallinity described the magnitude of the MES of bulk apatites, synthetic and biologic. That the mean value of apatite MES is linearly correlated with the microstrain parameter obtained by the Rietveld analysis of the apatite's X-ray diffraction pattern has been published.[16,27] The solid symbols of Figure 18

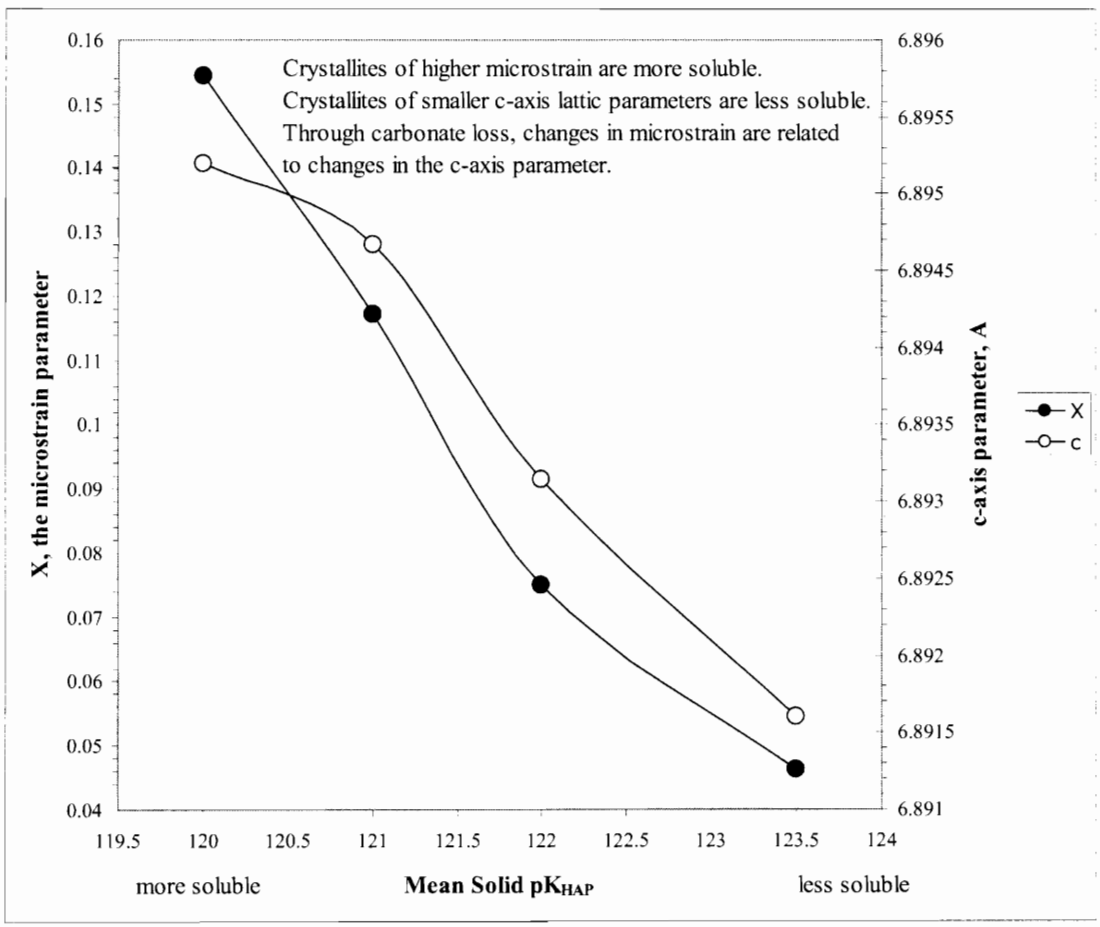

Figure 18. Mean solid pK_{HAP} vs. X (crystallinity) and c, the c-axis parameter.

show that this relationship holds even for fractionated portions of a particular apatite. The importance of this result is that the mean MES of not only bulk samples of a particular CAP, but also of its fractions can be predicted according to their microstrain.

The open symbols of Figure 18 suggest a reason behind which the change in crystallinity of the CAP powders in turn affects their MES. Shown is that a large MES corresponds with a large c-axis parameter. This is consistent with the view that crystallites without carbonate ion have a shorter c-axis lattice parameter, lower microstrain, and lower solubility than crystallites with carbonate. The decrease in carbonate of each of the three fraction of F1 was verified by assay, and is shown in Table III.

Figure 19 shows the somewhat surprising result that the residual, equilibrated, least-soluble crystallites are also the smallest crystallites. This might seem nonsensical if the general assumption is taken that smaller crystallites always have greater solubilities than larger crystallites. Although it is true that smaller crystallites have greater thermodynamic solubilities than larger crystallites if they are of identical material, the effect on solubility will not be significant unless the particles are small enough.

Consideration of a particle-size effect can be made with the Kelvin Equation,[33,34] a theoretical equation that describes the thermodynamic solubility of curved particles rel-

Table III. Carbonate assay results.

SAMPLE	*WEIGHT PERCENT CARBONATE*
F1	5.0
F114	5.0
F119	4.0
F121	3.5

Error in weight percent (reproducibility) = ± 0.3.

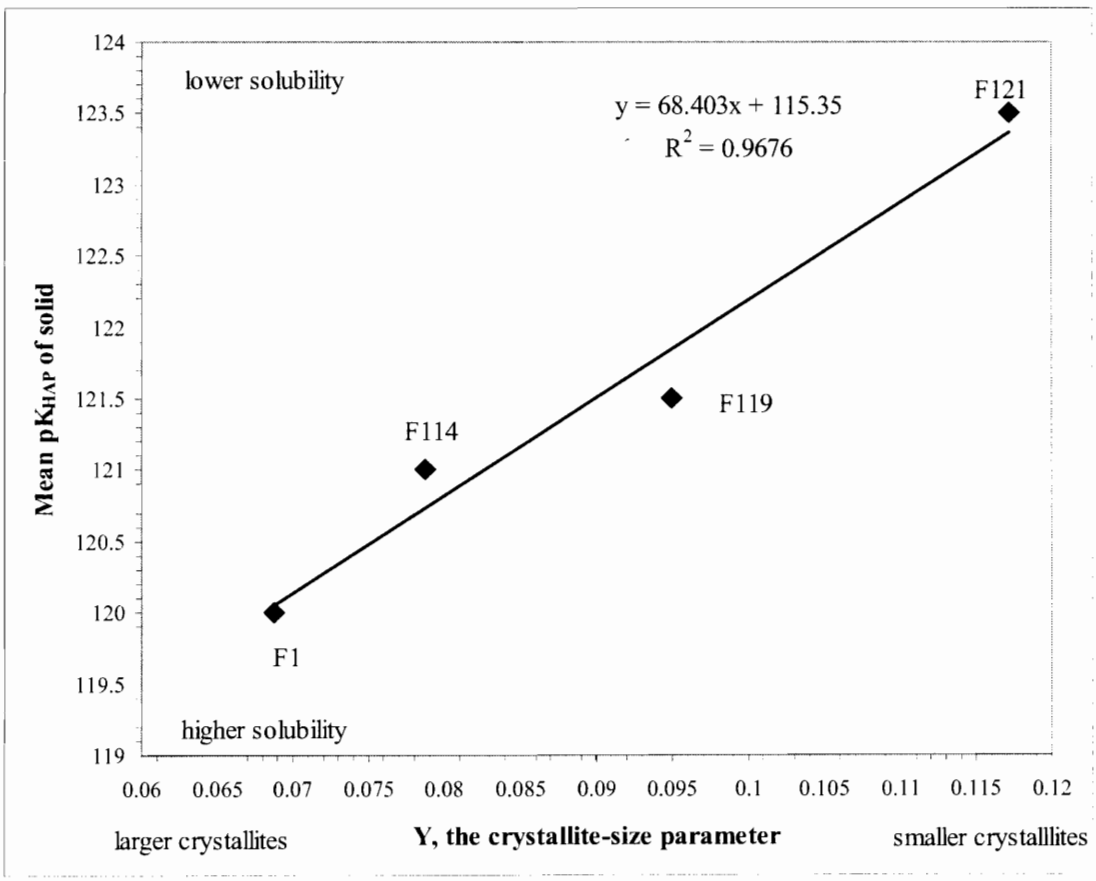

Figure 19. Mean solid pKHAP vs. Y, the crystallite-size parameter. The Kelvin Equation does not apply to this apatite system because here the most soluble crystals are not the smallest.

ative to flat ones. The Kelvin Equation is

$$\ln\left(\frac{a}{a_O}\right)=\frac{2V^S}{RT}\left(\frac{\gamma}{r}\right) \quad (9).$$

Here, a = solubility product of small particles; a_o = solubility product of large particles; V^s = molar volume of the solid, calculated from its lattice parameters; R = the universal gas constant; T = the absolute temperature; r = radius of the curved particle; and γ = surface tension.

However, quantitative use of the Kelvin Equation for ionic solids in partially saturated solutions is not trivial.[35] Surface energies of the solid-liquid interface are difficult to obtain; foreign solution ions can be absorbed to the solid as well as common ions in solution, which means that molar volumes and surface tensions of the solid change during the equilibration; and irregularities in shape have a greater impact on solubility than an effective radius.[34]

Nevertheless, Table IV presents some results by use of the Kelvin Equation. Published values[36,37] of apatite surface tension were used, and particle sizes were calculated for arbitrary increases in solubility product.

The calculated particle sizes, less than a few-hundred nanometers, are in the range where an increase in solubility is expected,[38] regardless of which of the two surface tensions is used. Very small sizes are required to increase the solubility product by factors of one hundred, one thousand, or more.

Table IV. Use of the Kelvin Equation in apatite systems.

Published surface tension, mJ/m^2	46.7	186
Arbitrary a/a_o	Calculated particle size, nm	Calculated particle size, nm
1.7	67	266
3	32	128
10	15	61
100	8	31
1000	5	20
10000	4	15

However, it must be kept in mind that the predicted increase would be for smaller particles compared to larger ones. Figure 19 does not show this expected increase; it shows its opposite. Interestingly, the particle sizes of the CAP powders used in this research (as estimated from the SEM photographs of Figures 4, 6, 8, and 10) are ~300 nm, which means that a modest increase in solubility product ($a/a_0 \approx 1.4$) could be expected between smaller particles compared to larger particles, not the more than 1000-fold increase between F1 (the larger particles) compared to F121 (the smaller particles).

Figure 19, then, is a counter-example to the thermodynamic case in which the slope of solubility versus inverse crystallite size would be opposite in sign. Thus we see that whereas solubility can be explained by microstrain (Figure 18), it cannot be explained universally by crystallite size. In other words, because of Figure 19, we see that crystallite size is not a good correlate of solubility for apatitic systems.

Nevertheless, Figure 19 is actually physically reasonable for apatite systems. If apatite is composed of a mixture of crystal domains of various sizes and metastable equilibrium solubilities (as is hypothesized by this laboratory), then there may exist small

crystallites with small solubilities as well as large crystallites with large solubilities. If this is the case, then the relationship of Figure 19 is not conceptually unreasonable based on the assumption of heterogeneity of sizes and solubilities of an apatite sample.

Figure 19 does not imply that before equilibration, smaller crystallites are less soluble. Nor does Figure 19 imply that larger crystallites disappear before smaller ones disappear. As dissolution occurs, the smaller crystallites, depending on their solubility, may or may not dissolve before the larger crystallites. In either case, the average crystallite size of the residual material will be smaller after dissolution if there is no solid reequilibration because particles become smaller as they dissolve. This is the physical explanation of Figure 19. (If reprecipitation or equilibration of solid phases did occur, the crystallite size of the remaining, undissolved residues would not be expected to be smaller than their bulk CAP; they would be expected to be larger due to "Ostwald Ripening,"[39] where small crystals disappear and recrystallize on larger crystals.)

Again, Figure 19 does suggest that a prediction of solubility cannot be done solely on crystallite size. Our laboratory has continued to affirm that the MES solubility distribution of an apatite is not a strong function of its particle size distribution.

In light of the data of this research, and the semiquantitative use of the Kelvin Equation, let us now reexamine two simplified views of the dissolution of apatite in terms of crystal properties as it reaches its MES.

View 1: Apatite's crystal size distribution accounts completely for its apparent solubility distribution. With this view, the fact that different percentages of a particular CAP dissolve in dissolution media of distinct solution ion activity product would be attributed solely to the CAP's crystal-size distribution. That is, the distribution is due to

the consequence of the Kelvin equation that thermodynamic solubilities of smaller particles are greater relative to larger ones of the same material.

If this were the case, we would expect that crystallite residues of the original CAP that were collected after equilibration in increasingly undersaturated dissolution media would be larger relative to more soluble crystallites because they are less soluble. In other words, the smaller crystallites would have dissolved while the larger ones remained. Figure 19, however, showed that the undissolved crystallites of the residues were in fact smaller, and Table II shows that the less-soluble residues had the highest specific surface areas. Not unexpectedly, smaller crystallite sizes give larger specific surface areas. It is concluded that these residuals remained undissolved because they are simply less soluble, or more crystalline, than the primary or secondary controls, regardless of the exposed surface area available for dissolution.

View 2: Apatite has a metastable equilibrium solubility distribution. Our laboratory has performed time-dependent studies of the MES distributions of apatite to show the kinetics of reaching MES.[25] While showing intersample variability, MES has normally been reached within days. In light of the observation that lower-soluble residues showed increasingly crystalline microstrain parameters, and that the primary and secondary controls seemed to behave as an algebraic sum of the solubilities of their dissolved and undissolved portions, it is hypothesized that apatite is indeed composed of independent domains of crystals that differ in solubility.

Conclusions

Apatite shows distributions of metastable equilibrium solubility (MES) irrespective of prior exposure to demineralizing solutions. Collected undissolved fractions of the original apatite that were reequilibrated in new demineralizing solutions showed their own MES distributions, which were systematically shifted toward lower-solubility values.

The more soluble portions of an apatite sample can be successively removed by equilibrating the apatite in increasingly dilute demineralizing solutions. Furthermore, bulk apatite not only appears to be a separable mixture of component fractions, but it behaves as a sum of these independent fractions, each of which has its own MES solubility distribution. Relative to the original apatite, the MES distributions of the re-equilibrated residues behaved simply as if the most-soluble parts of the original had been eliminated.

These observations support the view that during apatitic dissolution, the domains of highest microstrain independently dissolve while the less-soluble domains (those of lower microstrain) remain. Thus during the time frame of MES, the numerous domains of apatite (each with their own solubility) equilibrate solely with the dissolution medium but do not reequilibrate with each other.

Future work

There are many variables that may be involved, either alone or in combination, in the dissolution behavior of carbonated calcium hydroxyapatite and the achievement of a distribution of MES in time. These include degree of solution saturation, pH,

crystallinity, solution fluoride, adsorbed fluoride, slurry density, specific surface area. The strength of each factor has yet to be conclusively determined. In light of these unknowns, the following work is anticipated.

Obtain particle size distribution data of bulk apatite and apatite fractions. These data can be determined from transmission electron microscopy and x-ray diffraction data.[40] This will allow any contribution of the size distribution to either the MES distribution itself, or to the time required to reach the metastable equilibrium state to be factored out and independently considered.

Similar studies to this should be performed with apatites of larger and smaller solubility than F1. These studies will be done to further understand the importance of size distributions to MES phenomena; the relationships among solubility, microstrain, and crystallite size; and the principle of superposition as applied to the solubility of bulk apatite relative to its fractions.

As a preface to the next suggested experiment, note that Equation 5 is much more powerful and general than Equation 8. Equation 5 can be used with any CAP (a single preparation, or an arbitrary mixture of several preparations) as long as the weight fractions and the MES of these fractions are known. Equation 8 can be used with any CAP preparation with initially unknown component fractions.

An experiment to test the fact that apatitic domains equilibrate independently with the dissolution media is to combine known amounts of CAP samples, each of which has a known MES distribution. Create an arbitrary mixture of CAP with known amounts of these various synthesized samples. Perform MES-determination experiments on the mixture, and see if through Equation 5, the MES behavior of the bulk can be

mathematically reproduced from the knowledge of the behavior of its two or more fractions. A hypothetical example of a 50% mixture of two CAPs with narrow, non-overlapping MES is presented in Figure 20. (Fractionation may even need to be done to obtain CAPs A and B, which have such narrow distributions.)

Using Equation 5, if the fractional weights, x_i, of the component fractions are known, than Hypothesis 1 can be tested by measuring the MES of each of these fractions of any arbitrary mixture of CAP masses in the particular solution of interest, and then by comparing it to the MES of the bulk CAP in the same series of solutions.

Fractionation of carbonated apatite may lead to more than just findings of mathematical and mechanistic significance, but also to findings of biologic significance. Discontinued work[41,42] showed that harvested neonatal rabbit osteoclasts appeared to equally resorb pellet preparations of different mean MES. However, it is my opinion that the negligible discriminability of the osteoclasts during the experiments may have been because the two CAP preparations had significant overlap in their MES. Osteoclasts may still indeed show preference to larger differences in intrinsic metastable equilibrium solubility of the mineral. This knowledge might lead to an understanding of the relative importance of biologic and physicochemical factors in bone mineral diseases such as osteoporosis.

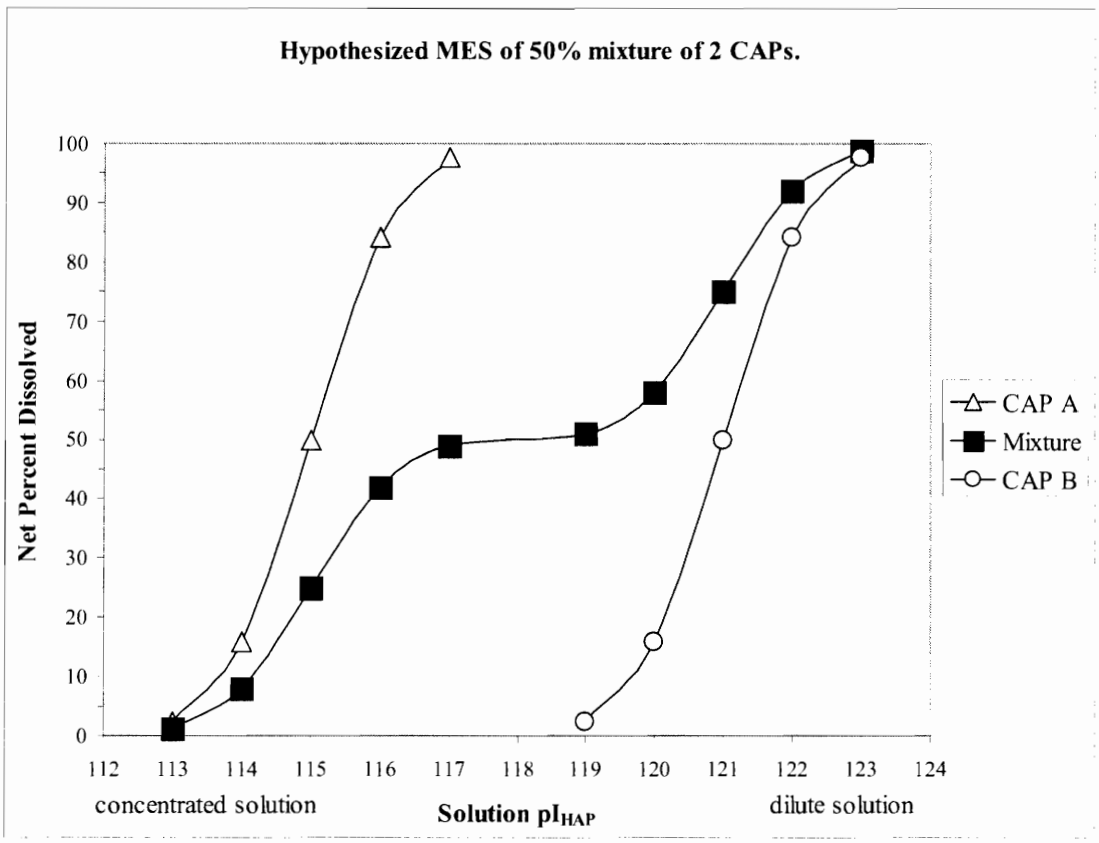

Figure 20. Hypothesized MES distribution profile of a nonoverlapping 50% mixture.

REFERENCES

1. LeGeros RZ. 1991. Calcium phosphates in oral biology and medicine. ed.: Karger.

2. Clark JS 1955. Solubility criteria for the existence of hydroxyapatite. Canad J Chem 33:1696-1700.

3. Levinskas GJ, Neuman, W.F. 1955. The solubility of bone mineral. I: Solubility studies of synthetic hydroxyapatite. J Phys Chem 59:164-168.

4. Brown WE. 1973. Solubilities of phosphate and other sparingly soluble compounds. In Griffith EL, Beeton, A., Spencer, J.M., Mitchell, D.T., editor Environmental Phosphorus Handbook, ed., New York: John Wiley and Sons. p 203-239.

5. Verbeeck RMH. 1986. Minerals in human enamel and dentin. In Driessens FCM WJ, editor Tooth development and caries, ed., Boca Raton: CRC Presss. p 95-152.

6. Rootare HM, Deitz, V.R., Carpenter, F.G. 1962. Solubility product phenomena in hydroxyapatite water systems. J Colloid Sci 17:179-206.

7. LaMer VK 1962. The solubility behavior of hydroxyapatite. J Phys Chem 66:973-978.

8. Moreno EC, Gregory, T.M., Brown, W.E. 1968. Preparation and solubility of hydroxyapatite. J Res Nat Bureau Standards 72A(suppl):773-782.

9. Wier DR, Chien, S.H., Black, C.A. 1971. Solubility of hydroxyapatite. Soil Sci 111:107-112.

10. Bell LC, Mika, H., Kruger, B.J. 1978. Synthetic hydroxyapatite solubility product and stoichiometry of dissolution. Arch Oral Biol 23:329-336.

11. Verbeeck RMH, Steyaer, H., Thun, H.P., Verbeeck, F. 1980. Solubility of synthetic calcium hydroxyapatite. JCS Faraday I 78:209-219.

12. Young RA, Holcomb, D.W. 1982. Variability of hydroxyapatite preparation. Calcif Tissue Int 34:S17-S32.

13. Hsu J, Fox, J.L., Higuchi, W.I., Powell, G.L., Otsuka, M., Baig, A., LeGeros, R.Z. 1994. Metastable Equilibrium Solubility Behavior of Carbonated Apatites. J Colloid Interface Sci 167(2):414-423.

14. Baig AA, Fox, J.L., Wang, Z., Higuchi, W.I., Miller, S.C., Barry, A.M., Otsuka, M. 1999. Metastable Equilibrium Solubility Behavior of Bone Mineral. Calcif Tissue Int 64(4):329-339.

15. Patel PR, Brown, W.E. 1975. Thermodynamic solubility product of human tooth enamel: powdered sample. J Dent Res 54:728-736.

16. Baig AA, Fox, J.L., Young, R.A., Higuchi, W.I., Wang, Z., Hsu, J., Chhettry, A., Zhuang, H., Otsuka, M. 1999. Relationships between carbonated apatite solubility, crystallite size, and microstrain parameters. Calcif Tissue Int 64:437.

17. Amis EJ, Rumble Jr., J. 2003. Certificate of Analysis, Standard Reference Material 2910, Calcium Hydroxyapatite. ed., Gaithersburg, MD: National Institute of Standards and Technology.

18. Chhettry A, Wang, Z., Fox, J.L., Hsu, J., Baig, A.A., Zhuang, H., Higuchi, W.I. 1999. Use of dicalcium phosphate dihydrate as a probe in an approach for the accurate calculations of solution equilibria in buffered calcium phosphate systems. J Colloid Interface Sci 218(1):47-56.

19. Brunauer S, Emmett, P.H., Teller, E. 1938. Adsorption of Gases in Multimolecular Layers. J Am Chem Soc 60:309-319.

20. Zhuang H, Baig, A.A., Chhettry, A., Barry, A.M., Fox, J.L., Higuchi, W.I. 1999. Threshold concentration for solution fluoride influencing biomineral solubility. J Dental Research (Special):Abstract #1865.

21. Zhuang H, Baig, A.A., Fox, J.L., Wang, Z., Colby, S.J., Chhettrry, A., Higuchi, W.I. 2000. Metastable equillibrium solubility behavior of carbonated apatites in the presence of solution fluoride. J Colloid Interface Sci 222(1):90-96.

22. Chhettry A, Baig, A.A., Fox, J.L., Higuchi, W.I. 1999. Composition of the Surface Complex Governing Carbonated Apatite Dissolution. J Dental Research (Special):Abstract #1866.

23. Heslop DD, Bi, Y., Baig, A.A., Higuchi, W.I. 2003. Metastable Equililbrium Solubility Behavior of Carbonated Apatite in the Presence of Solution Strontium. Calcif Tissue Int 71(1):72-85.

24. Chhettry A, Wang, Z., Hsu, J., Fox, J.L., Baig, A.A., Barry, A.M., Zhuang, H., Otsuka, M., Higuchi, W.I. 1999. Metastable Equilibrium Solubility Distribution

of Carbonated Apatite as a Function of Solution Composition. J Colloid Interface Sci 218(1):57-67.

25. Chhettry A, Wang, Z., Baig, A.A., Fox, J.L., Higuchi, W.I. 1998. Critical evaluation of surface complex governing carbonated apatite dissolution. J Dental Research 77(Special):Abstract #1422.

26. Barry AM, Baig, A.A., Zhuang, H., Fox, J.L., Higuchi, W.I., Otsuka, M. 1999. A proposed methodology for bone mineral solubility determination. J Dental Research (Special):Abstract #1863.

27. Heslop DD, Bi, Y., Baig, A.A., Otsuka, M., Higuchi, W.I. 2005. A comparitive study of the metastable equilibrium solubility behavior of high-crystallinity and low-crystallinity carbonated apatites using pH and solution strontium as independent variables. J Colloid Sci 289(1):14-25.

28. Pratt JW, Baig, A.A., Wang, Z., Fox, J.L., Higuchi, W.I. 1998. Effect of heat-treatment on solubility behavior of carbonated apatite. J Dental Research 77(Special Issue A):Abstract #1424.

29. Wang Z. 1994. Dissolution Kinetics of carbonated apatite and effects of solution ions. Pharmaceutics and Pharmaceutical Chemistry, ed., Salt Lake City: University of Utah. p 195.

30. Barry AB, Baig, A.A., Miller, S.C., Higuchi, W.I. 2002. Effect of Age on Rat Bone Solubility and Crystallinity. Calcif Tissue Int 71(2):167-171.

31. Arends J, Jongebloed, W.L. 1981. Apatite single crystals. Formation, dissolution and influence of CO_3^{2-} ions. Recl Trav Chim Pays-Bas 100:3-9.

32. Barry AB, Zhuang, Z., Baig, A.A., Higuchi, W.I. 2003. Effect of Fluoride Pretreatment on the Solubility of Synthetic Carbonated Apatite. Calcif Tissue Int 72(3):236-242.

33. Castellan GW. 1983. Physical Chemistry. 3rd ed., CA: Addison Wesley. p 415.

34. Hiemenz PC, Rajagopalan, R. 1997. Principles of Colloid and Surface Chemistry. 3rd ed., New York, NY: Marcel Dekker. p 261-264.

35. Rideal EK. 1930. The Liquid-Solid Interface. An Introduction to Surface Chemistry, 2° ed., Cambridge, UK: University Press. p 253-255.

36. Lopes MA, Monteiro, F.J., Santos, J.D., Serro, A.P., Saramago, B. 1999. Hydrophobicity, surface tension, and zeta potential measurements of glass-reinforced hydroxyapatite composites. J Biomed Mater Res 45:370-375.

37. Madsen HEL 1975. Ionic concentrations in calcium phosphate solutions. II. The solubility of hydroxylapatite in water or salt solutions at 37 °C. Acta Chemica Scandinavica A 29(8):745-748.

38. Bancroft WD. 1926. Coalescence. Applied Colloid Chemistry-General Theory, 2° ed., New York, NY: McGraw-Hill Book Company, Inc. p 173-199.

39. Dean RB. 1948. Modern Colloids. ed., New York, NY: D. Van Nostrand Company, Inc.

40. Gomonnai AV, Azhniuk, Yu M., Vysochanskii, Yu M., Kikineshi, A.A., Kis-Varga, M., Daroczy, L., Prits, I.P., Voynarovych, I.M. 2003. Raman and x-ray diffraction studies of nanometric $Sn_2P_2S_6$ crystals. J Phys: Condens Matter 15:6381-6393.

41. Barry A, Baig, A.A., Wang, Z., Fox, J.L., Higuchi, W.I., Otsuka, M. 1998. A synthetic substrate system to explore osteoclast activity *in vitro*. J Dental Research 77(Special):Abstract #43.

42. Barry AB. 2003. Metastable equilibrium solubility of biominerals: biological and physicochemical considerations. Pharmaceutics and Pharmaceutical Chemistry, ed., Salt Lake City: University of Utah. p 145.